

# Immunoglobulin G1 Fc glycosylation as an early hallmark of severe COVID-19

1 **Tamas Pongracz<sup>1,\*</sup>, Jan Nouta<sup>1</sup>, Wenjun Wang<sup>1</sup>, Krista. E. van Meijgaarden<sup>4</sup>, Federica Linty<sup>2,3</sup>,**  
2 **Gestur Vidarsson<sup>2,3</sup>, Simone A. Joosten<sup>4</sup>, Tom H. M. Ottenhoff<sup>4</sup>, Cornelis H. Hokke<sup>5</sup>, Jutte J. C.**  
3 **de Vries<sup>6</sup>, Sescu M. Arbous<sup>7</sup>, Anna H. E. Roukens<sup>7</sup>, Manfred Wuhrer<sup>1</sup> in collaboration with**  
4 **BEAT-COVID<sup>#</sup> and COVID-19<sup>&</sup> groups**

5 <sup>1</sup>Center for Proteomics and Metabolomics, Leiden University Medical Center, Leiden, Netherlands

6 <sup>2</sup>Dept. of Experimental Immunohematology, Sanquin Research, Amsterdam, Netherlands

7 <sup>3</sup>Landsteiner Laboratory, Amsterdam University Medical Center, Amsterdam, Netherlands

8 <sup>4</sup>Dept. of Infectious Diseases, Leiden University Medical Center, Leiden, Netherlands

9 <sup>5</sup>Dept. of Parasitology, Leiden University Medical Center, Leiden, Netherlands

10 <sup>6</sup>Dept. of Medical Microbiology, Leiden University Medical Center, Leiden, Netherlands

11 <sup>7</sup>Dept. of Intensive Care, Leiden University Medical Center, Leiden, Netherlands

12 **#BEAT-COVID group** (in alphabetical order, investigators): B. M. van den Berg<sup>2</sup>, S. Cannegieter<sup>3</sup>,  
13 C. M. Cobbaert<sup>4</sup>, A. van der Does<sup>5</sup>, J. J. M. van Dongen<sup>6</sup>, H. C. J. Eikenboom<sup>7</sup>, M. C. M. Feltkamp<sup>8</sup>,  
14 A. Geluk<sup>9</sup>, J. J. Goeman<sup>10</sup>, M. Giera<sup>11</sup>, T. Hankemeier<sup>12</sup>, M. H. M. Heemskerck<sup>13</sup>, P. S. Hiemstra<sup>5</sup>, J. J.  
15 Janse<sup>14</sup>, S. P. Jochems<sup>14</sup>, M. Kikkert<sup>8</sup>, L. Lamont<sup>12</sup>, J. Manniën<sup>10</sup>, M. R. del Prado<sup>1</sup>, N. Queralt  
16 Rosinach<sup>15</sup>, M. Roostenberg<sup>14</sup>, M. Roos<sup>15</sup>, H. H. Smits<sup>14</sup>, E. J. Snijder<sup>8</sup>, F. J. T. Staal<sup>6</sup>, L. A. Trouw<sup>6</sup>,  
17 R. Tsonaka<sup>10</sup>, A. Verhoeven<sup>11</sup>, L. G. Visser<sup>9</sup>, J. J. C. de Vries<sup>8</sup>, D. J. van Westerloo<sup>1</sup>, J. Wigbers<sup>1</sup>, H.  
18 J. van der Wijk<sup>10</sup>, R. C. van Wissen<sup>4</sup>, M. Yazdanbakhsh<sup>14</sup>, M. Zlei<sup>6</sup>

19 <sup>1</sup>Dept. of Intensive Care, Leiden University Medical Center, Leiden, Netherlands

20 <sup>2</sup>Dept. of Internal Medicine, Nephrology, Leiden University Medical Center, Leiden, Netherlands

21 <sup>2</sup>Dept. of Clinical Epidemiology, Leiden University Medical Center, Leiden, Netherlands

22 <sup>4</sup>Dept. of Clinical Chemistry, Leiden University Medical Center, Leiden, Netherlands

23 <sup>5</sup>Dept. of Pulmonary Medicine, Leiden University Medical Center, Leiden, Netherlands

24 <sup>6</sup>Dept. of Immunology, Leiden University Medical Center, Leiden, Netherlands

25 <sup>7</sup>Dept. of Internal Medicine, Thrombosis and Hemostasis, Leiden University Medical Center,  
26 Leiden, Netherlands

27 <sup>8</sup>Dept. of Medical Microbiology, Leiden University Medical Center, Leiden, Netherlands

28 <sup>9</sup>Dept. of Infectious Diseases, Leiden University Medical Center, Leiden, Netherlands

29 <sup>10</sup>Dept. of Biomedical Data Sciences, Leiden University Medical Center, Leiden, Netherlands

30 <sup>11</sup>Center for Proteomics and Metabolomics, Leiden University Medical Center, Leiden, Netherlands

31 <sup>12</sup>Dept. of Analytical Biosciences, Leiden Academic Centre for Drug Research, Leiden, Netherlands

32 <sup>13</sup>Dept. of Hematology, Leiden University Medical Center, Leiden, Netherlands

33 <sup>14</sup>Dept. of Parasitology, Leiden University Medical Center, Leiden, Netherlands

34 <sup>15</sup>Dept. of Human Genetics, Leiden University Medical Center, Leiden, Netherlands

35 **&COVID-19 group** (in alphabetical order, investigators):

36 M. Baysan<sup>2,3</sup>, M. G. J. de Boer<sup>4</sup>, A. G. van der Bom<sup>3</sup>, O. M. Dekkers<sup>3</sup>, A. M. Eikenboom<sup>3</sup>, S. B. ter  
37 Haar<sup>3</sup>, L. Heerdink<sup>3</sup>, L. J. van Heurn<sup>3</sup>, I. de Jonge<sup>3</sup>, W. Lijfering<sup>3</sup>, R. Meier<sup>1</sup>, J. A. Oud<sup>1</sup>, F. Rosendaal<sup>3</sup>,  
38 A. G. L. Toppenberg<sup>3</sup>, J. Uzorka<sup>4</sup>, A. A. van IJlzinga Veenstra, J. Wigbers<sup>2</sup>, J. M. Wubbolts<sup>4</sup>

39 <sup>1</sup>Dept. of Hematology, Leiden University Medical Center, Leiden, Netherlands

40 <sup>2</sup>Dept. of Intensive Care, Leiden University Medical Center, Leiden, Netherlands

41 <sup>3</sup>Dept. of Clinical Epidemiology, Leiden University Medical Center, Leiden, Netherlands

42 <sup>4</sup>Dept. of Infectious Diseases, Leiden University Medical Center, Leiden, Netherlands

43 **\*Correspondence:**

44 Tamas Pongracz

45 Albinusdreef 2, 2223ZA, Leiden, Netherlands

46 Tel: +31 71 526 8701

47 [t.pongracz@lumc.nl](mailto:t.pongracz@lumc.nl)

48 **Abstract**

49 **Background**

50 Immunoglobulin G1 (IgG1) effector functions are impacted by the structure of fragment crystallizable  
51 (Fc) tail-linked *N*-glycans. Low fucosylation levels on severe acute respiratory syndrome coronavirus  
52 2 (SARS-CoV-2) spike protein specific (anti-S) IgG1 has been described as a hallmark of severe  
53 coronavirus disease 2019 (COVID-19) and may lead to activation of macrophages via immune  
54 complexes thereby promoting inflammatory responses, altogether suggesting involvement of IgG1 Fc  
55 glycosylation modulated immune mechanisms in COVID-19.

56 **Methods**

57 In this prospective, observational single center cohort study, IgG1 Fc glycosylation was analyzed by  
58 liquid chromatography – mass spectrometry following affinity capturing from serial plasma samples  
59 of 159 SARS-CoV-2 infected patients.

60 **Findings**

61 At baseline close to disease onset, anti-S IgG1 glycosylation was highly skewed when compared to  
62 total plasma IgG1. A rapid, general reduction in glycosylation skewing was observed during the disease  
63 course. Low anti-S IgG1 galactosylation and sialylation as well as high bisection were early hallmarks  
64 of disease severity, whilst high galactosylation and sialylation and low bisection were found in patients  
65 with low disease severity. In line with these observations, anti-S IgG1 glycosylation correlated with  
66 various inflammatory markers.

67 **Interpretation**

68 Association of low galactosylation, sialylation as well as high bisection with disease severity suggests  
69 that Fc-glycan modulated interactions contribute to disease mechanism. Further studies are needed to  
70 understand how anti-S IgG1 glycosylation may contribute to disease mechanism and to evaluate its  
71 biomarker potential.

72 **Funding**

73 This project received funding from the European Commission's Horizon2020 research and innovation  
74 program for H2020-MSCA-ITN IMforFUTURE, under grant agreement number 721815.

75 **Keywords: IgG glycosylation; anti-Spike IgG; SARS-CoV-2; COVID-19; coronavirus**

76 **Research in context**

77 **Evidence before this study**

78 Antibody glycosylation against the spike (S) protein of patients infected with severe acute respiratory  
79 syndrome SARS-CoV-2 has been reported as a potentially important determinant of COVID-19  
80 disease severity. Studies have hitherto focused on afucosylation, a modification on immunoglobulin  
81 G1 (IgG) Fc-tail-linked *N*-glycans that enhances effector functions. Most of these studies featured  
82 limited sample numbers or were imperfectly matched with respect to demographic and other important  
83 confounding factors. Our lab has contributed to some of these studies, and we additionally searched  
84 for research articles on PubMed and Google Scholar from January 2020 to October 2021. To date, only  
85 two groups studied anti-S IgG1 glycosylation, which resulted in overall three publications found.  
86 However, none of these groups found a severity marker between hospitalized non-ICU and ICU  
87 patients or studied dynamic changes. Instead, exclusively fucosylation at the first available timepoint  
88 has been associated with disease severity between severely ill inpatients and mild outpatients.

## 89 **Added value of this study**

90 In this prospective, observational single center cohort study, we investigated the severity marker  
91 potential of anti-S IgG1 glycosylation in severe and mild hospitalized COVID-19 cases, and correlated  
92 these findings with numerous inflammation and clinical markers. Our study reveals low galactosylation  
93 and sialylation as well as high bisection on anti-S IgG1 as early hallmarks of severe COVID-19, after  
94 correction for age and sex effects. In line with these observations, anti-S IgG1 glycosylation correlated  
95 with many inflammatory markers. As days since onset is one of the major confounders of anti-S IgG1  
96 glycosylation due to its highly dynamic nature, we additionally confirmed our findings in time-matched  
97 patient subgroups. We believe anti-S IgG1 glycosylation may be applicable for patient stratification  
98 upon hospitalization.

## 99 **Implications of all the available evidence**

100 Demographic factors as well as temporal differences should be taken into consideration when  
101 analyzing IgG1 glycosylation of COVID-19 patients. Anti-S IgG1 glycosylation is highly dynamic,  
102 but is a promising early severity marker in COVID-19.

## 103 **1 Introduction**

104 The current global coronavirus disease 19 (COVID-19) pandemic caused by the novel coronavirus  
105 severe acute respiratory syndrome coronavirus 2 (SARS-CoV-2) has been leading to extensive  
106 hospitalizations worldwide.<sup>1</sup> To date, more than 253 million infections and more than 5 million deaths  
107 have been reported.<sup>2</sup> SARS-CoV-2 is an enveloped virus and its uptake by target cells in the respiratory  
108 tract is mediated by the spike glycoprotein.<sup>1</sup> Interestingly, most infected people clear the virus with  
109 mild symptoms, whilst around 20% of the adult cases are characterized by severe, sometimes life-  
110 threatening conditions.<sup>3</sup> Approximately 7-10 days after symptom onset, seroconversion occurs with  
111 immunoglobulin M (IgM) and A (IgA), and G (IgG) antibodies against the spike protein.<sup>4</sup> These  
112 antibodies can form immune complexes with viral particles and thereby neutralize the virus and  
113 mediate clearance, but are also capable of aggravating the disease.<sup>5-7</sup>

114 IgG exerts effector functions via the activation of complement or fragment crystallizable (Fc) gamma  
115 receptors (FcγR) on immune cells.<sup>8</sup> Various effector functions of IgG are steered by the *N*-glycan  
116 moiety attached to the highly conserved N297 glycosylation sites within both C<sub>H</sub>2 domains of the Fc  
117 tail.<sup>9,10</sup> Specifically, afucosylated IgG1 shows increased affinity to the activating FcγRIIIa receptor,  
118 hence leading to enhanced antibody-dependent cellular cytotoxicity (ADCC).<sup>10,11</sup> Galactosylated IgG1  
119 shows increased hexamerization, C1q binding and complement activation.<sup>12</sup>

120 Recent reports have indicated that the high inter-individual variability in COVID-19 disease severity<sup>3</sup>  
121 may partly be explained by low Fc fucosylation of anti-SARS-CoV-2 spike protein-specific (anti-S)  
122 IgG1. The lack of core fucose on these specific antibodies early on during disease points to their  
123 potential proinflammatory role in severe illness.<sup>6,13,14</sup> Literature suggests, that in particular membrane-  
124 embedded foreign antigens, such as the SARS-CoV-2 spike protein, induce low fucosylated IgG1  
125 responses, which in combination with high titers may lead to excessive macrophage activation and  
126 drive COVID-19 associated pathology including acute respiratory distress syndrome.<sup>6,13</sup>

127 Here, we study the dynamics of IgG1 Fc glycosylation and its association with clinical parameters in  
128 a longitudinal cohort of 159 hospitalized COVID-19 patients, analyzing a total of 1300 longitudinal  
129 patient samples. We report on the association of early anti-S IgG1 glycosylation signatures with disease  
130 severity and various inflammatory markers, indicating its biomarker potential.

## 131 **2 Methods**

### 132 **2.1 Chemicals, reagents and enzymes**

133 Type I Ultrapure Water was produced by an ELGA Purelab Ultra system (Elga LabWater, High  
134 Wycombe, United Kingdom) and used to create solutions throughout. Ammonium bicarbonate,  
135 potassium chloride, formic acid, tolylsulfonyl phenylalanyl chloromethyl ketone-treated trypsin from  
136 bovine pancreas was obtained from Sigma-Aldrich (Steinheim, Germany). Trifluoroacetic acid,  
137 disodium hydrogen phosphate dihydrate, potassium dihydrogen phosphate, and sodium chloride were  
138 purchased from Merck (Darmstadt, Germany). HPLC-supra-gradient acetonitrile was obtained from  
139 Biosolve (Valkenswaard, The Netherlands). The Visucon-F pooled healthy human plasma standard  
140 originated from Affinity Biologicals (Ancaster, Canada). Protein G Sepharose 4 Fast Flow beads were  
141 obtained from GE Healthcare (Uppsala, Sweden). Recombinant trimerized spike protein was prepared  
142 as described.<sup>15</sup>

### 143 **2.2 Study cohort**

144 BEAT-COVID-19 is a prospective, observational single center cohort study established at Leiden  
145 University Medical Center, with longitudinal plasma samples of 159 PCR-confirmed SARS-CoV-2  
146 infected hospitalized patients that were collected during the first and second wave of the pandemic  
147 (between May 2020 and October 2020) (**Table 1, Table S1, Figure S1**). After informed consent was  
148 obtained from the patient or his/her relatives, longitudinal sampling was performed for the duration of  
149 the hospital admission, and one convalescent sample was obtained at the outpatient follow-up  
150 appointment, which was scheduled six weeks after hospital discharge. Statistical sample size  
151 calculation was not performed, the sample size was determined based on availability. The Medical  
152 Ethics Committee Leiden-Den Haag-Delft (NL73740.058.20) approved the study. The trial was  
153 registered in the Dutch Trial Registry (NL8589). The study complied with the latest version of the  
154 Declaration of Helsinki.

### 155 **2.3 Sample preparation for IgG Fc glycosylation analysis**

156 Anti-S IgG was captured using a setup that resembles a conventional ELISA: IgGs were affinity-  
157 captured from plasma using recombinant trimerized spike-protein-coated Maxisorp NUNC-Immuno  
158 plate (Thermo Fisher Scientific, Roskilde, Denmark), whereas total IgG was affinity-captured using  
159 protein G Sepharose Fast Flow 4 beads, as described previously.<sup>13,16</sup> Antibodies were eluted using 100  
160 mM formic acid and the samples were dried by vacuum centrifugation. Samples were reconstituted in  
161 25 mM ammonium bicarbonate and subjected to tryptic cleavage, as described elsewhere.<sup>16</sup> Samples

162 belonging to a single patient were prepared and measured consecutively on the same plate, except for  
163 follow-up samples after hospitalization period. On each plate, at least 3 Visucon-F plasma standards  
164 (dating pre-COVID-19) and 3 blanks were included.

## 165 **2.4 IgG Fc glycosylation analysis**

166 Glycopeptides were separated and detected using an Ultimate 3000 high-performance liquid  
167 chromatography (HPLC) system (Thermo Fisher Scientific, Waltham, MA) hyphenated to an Impact  
168 quadrupole time-of-flight mass spectrometer (Bruker Daltonics, Billerica, MA), as described.<sup>16</sup>

## 169 **2.5 Liquid chromatograph – mass spectrometry data processing**

170 MzXML files were generated from raw liquid chromatograph – mass spectrometry (LC-MS) spectra.  
171 An in-house developed software, LaCyTools was used for the alignment and targeted extraction of raw  
172 data.<sup>17</sup> Alignment was performed based on the average retention time of minimum three abundant IgG1  
173 glycoforms. The targeted extraction list included analytes of the 2<sup>+</sup> and 3<sup>+</sup> charge states and was based  
174 on manual annotation of the mass spectra as well as on literature.<sup>18,19</sup> A pre-COVID-19 plasma pool  
175 (Visucon-F) was measured in triplicate in each plate to assess method robustness and was as well used  
176 as negative control. All spectra below the average intensity plus three times the standard deviation of  
177 negative controls was excluded from further analysis. Signals were integrated by covering a minimum  
178 of 95% of the area of the isotopic envelope of glycopeptide peaks. Inclusion of an analyte for the final  
179 data analysis was based on quality criteria such as signal-to-noise (> 9), isotopic pattern quality (< 25%  
180 deviation from the theoretical isotopic pattern), and mass error (within a  $\pm 20$  ppm range). Furthermore,  
181 analytes that were present in at least 1 out of 4 anti-S IgG1 spectra (25%) were included in the final  
182 analysis.

## 183 **2.6 Cytokine measurements by cytometric bead array**

184 Circulating cytokine and chemokine levels were determined in serum using commercially available  
185 bead based multiplex assays using the BioPlex 100 system for acquisition as previously described.<sup>20</sup>  
186 Standard curves were included in the kits and, in addition, a pooled serum sample of 4 hospital admitted  
187 COVID-19 patients was included as internal reference in all assays. Four commercially available kits  
188 were used: Bio-Plex Pro™ Human Cytokine Screening Panel 48-plex, Bio-Plex Pro™ Human  
189 Chemokine Panel 40-Plex, Bio-Plex Pro™ Human Inflammation Panel 1 and 37-Plex; Bio-Plex Pro™  
190 Human Th17 panel (IL-17F, IL-21, IL-23, IL-25, IL-31, IL-33) (all obtained from Bio-Rad,  
191 Veenendaal, The Netherlands).

## 192 **2.7 Antibody titer measurement**

193 Semi-quantitative detection of SARS-CoV-2 anti-nucleocapsid (N) protein IgG was performed on the  
194 Abbott Architect platform.<sup>21-23</sup> In this antibody chemiluminescent microparticle immunoassay (CMIA)  
195 test, the SARS-CoV-2 antigen coated paramagnetic microparticles bind to the IgG antibodies that  
196 attach to the viral nucleocapsid protein in human serum samples. The Sample/Calibrator index values  
197 of chemiluminescence in relative light units (RLU) of 1.40 (IgG assay) respectively 1.00 (IgM assay)  
198 and above were considered as positive per the manufacturer's instructions.

199 Quantitative detection of SARS-CoV-2 anti-S1/S2 IgG antibodies was performed using the DiaSorin  
200 LIAISON platform. The CLIA assay consists of paramagnetic microparticles coated with distally  
201 biotinylated S1 and S2 fragments of the viral surface spike protein. RLU's proportional to the sample's  
202 anti-S1/S2 IgG levels are converted to AU/mL based on a standardized master curve.



203 Semi-quantitative detection of SARS-CoV-2 anti-RBD IgM antibodies was performed using the  
204 Wantai IgM-ELISA (CE-IVD) kit (Sanbio).<sup>24</sup> Briefly, the IgM u-chain capture method was used to  
205 detect IgM antibodies using a double-antigen sandwich immunoassay using mammalian cell-expressed  
206 recombinant antigens containing the RBD of the spike protein of SARS-CoV-2 and the immobilized  
207 and horseradish peroxidase-conjugated antigen. Sample/Cut-off index OD values of 1 and higher were  
208 considered positive per the manufacturer's instructions.

209 Semi-quantitative detection of SARS-CoV-2 anti-S1 IgA antibodies was performed using the  
210 Euroimmun IgA 2-step ELISA.<sup>25</sup> Ratio values of 1.1 and higher were considered positive per the  
211 manufacturer's instructions.

## 212 **2.8 Severity score calculation**

213 The severity score is based on the 4C mortality score.<sup>26</sup> The 4C mortality score is a prediction score  
214 calculated at admission, and the severity score calculated in our cohort represents the daily clinical  
215 disease severity, and thus is dependent on parameters that can change over time. Therefore, the fixed  
216 parameters of the 4C score were removed (i.e. age, sex at birth, number of comorbidities). Daily oxygen  
217 flow for non-ICU patients (L/min) and p/f ratio (kPa) and FiO<sub>2</sub> (%) for ICU patients were added to our  
218 severity score (**Table S2**).

## 219 **2.9 Statistical analysis**

220 Relative intensity of each glycopeptide species in the final analyte list was calculated by normalizing  
221 to the sum of their total areas (**Table S3**). Structurally similar glycopeptide species were used for the  
222 calculation of derived traits fucosylation, bisection, galactosylation and sialylation (**Table S4**). Anti-S  
223 and total IgG1 glycosylation traits were compared using a Wilcoxon signed-rank test (**Figure 1, Table**  
224 **S5**), while a Wilcoxon rank-sum test was used to compare non-ICU and ICU patients as well as severity  
225 score groups (**Figure 3-4; Table S6-7; Figure S3, Figure S9-10**). To account for multiple testing, *p*-  
226 values of the Wilcoxon-tests have been corrected by the Benjamini-Hochberg procedure to 5% FDR  
227 in each statistical question (**Table S5-7**). Spearman's correlation was used to explore associations  
228 between glycosylation traits and age (**Figure S2**), as well as between glycosylation traits and  
229 inflammatory markers and titers (**Figure 5, Table S8**). To assess method repeatability, the inter-plate  
230 variation for the 14 analytes included in the final analysis was calculated for the standards, which was  
231 2.4%. All statistical analyses and visualizations were performed in R, version 4.1.0 (R Foundation for  
232 Statistical Computing, Vienna, Austria) and RStudio, version 1.4.1717 (RStudio, Boston, MA).

## 233 **2.10 Role of funding source**

234 The funders had no role in study design, data collection, data analysis, data interpretation, or writing  
235 of the report.

## 236 **3 Results**

237 Both anti-S and total IgG1 glycosylation signature of 159 COVID-19 patients (39 female and 119  
238 male) and corresponding timepoints were analyzed during their entire hospitalization period. The  
239 patient demographics and the comprehensive cohort characteristics are presented in **Table 1** and **Table**  
240 **S1**, respectively. Follow-up samples after hospital discharge were available for 19 patients (**Table S1,**  
241 **Figure S5**). LC-MS was employed to analyze Fc glycosylation on the glycopeptide level after tryptic  
242 digestion, which allowed the identification of 14 glycoforms. The found glycoforms were consistent  
243 with previous reports on anti-S IgG1 glycosylation<sup>13,14</sup>, from which fucosylation, bisection,

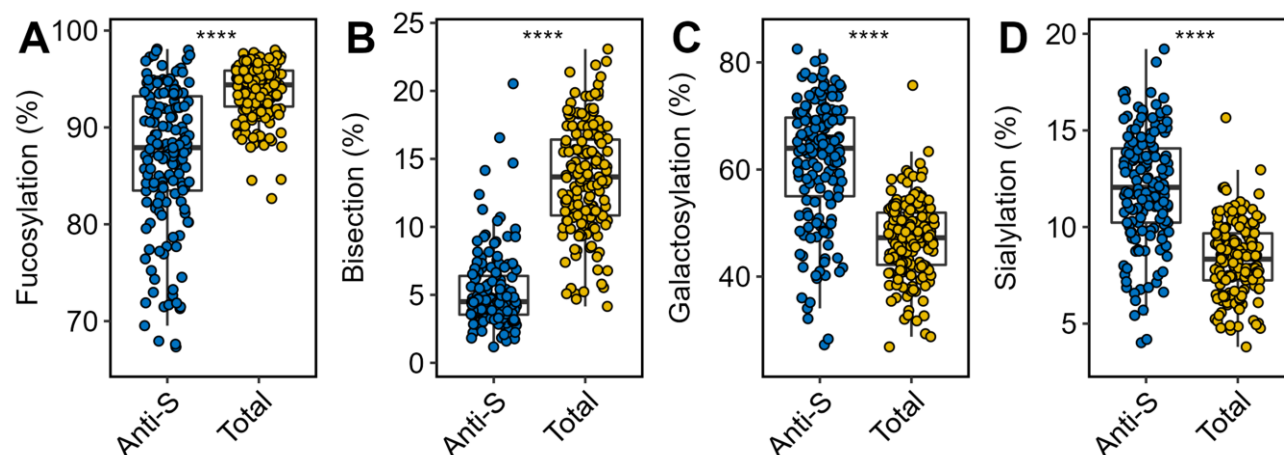
244 galactosylation and sialylation were calculated (**Table S3-4**). Overall, a total of 650 total IgG1 and 650  
245 anti-S IgG1 glycosylation profiles were determined.

246 **Table 1. Baseline patient characteristics.** Median and interquartile ranges are shown unless indicated otherwise. The sex  
247 of one patient is unknown (not shown).

	ICU (n=77)	non-ICU (n=82)
Age	65 (59-71)	66.5 (54-74.5)
Female, n (%)	18 (23)	21 (26)
Male, n (%)	59 (77)	60 (74)
Severity score	12 (10-14)	3 (2-4)
Days since symptom onset	15.5 (12-22)	13 (10-16)

### 248 3.1 Anti-S IgG1 Fc glycosylation of COVID-19 patients is skewed

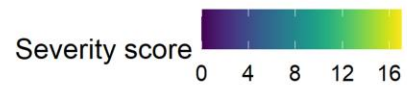
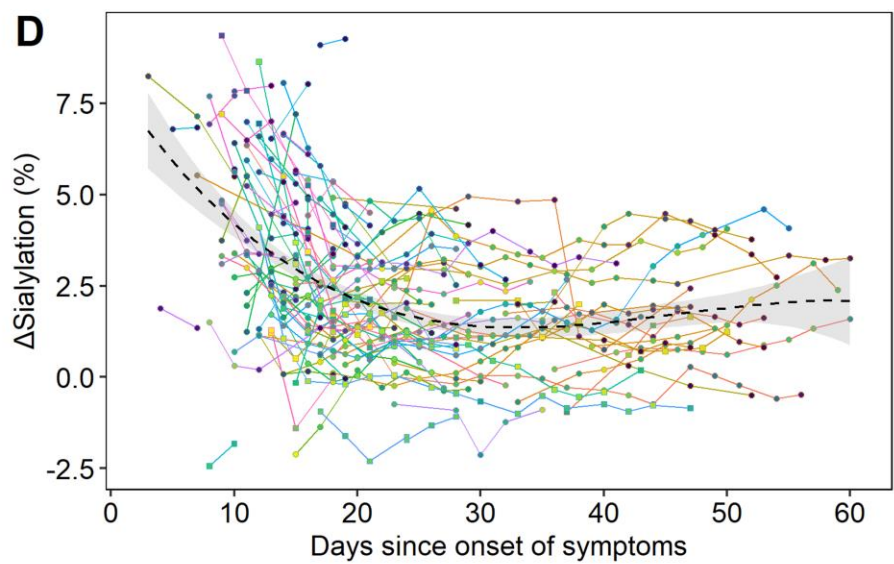
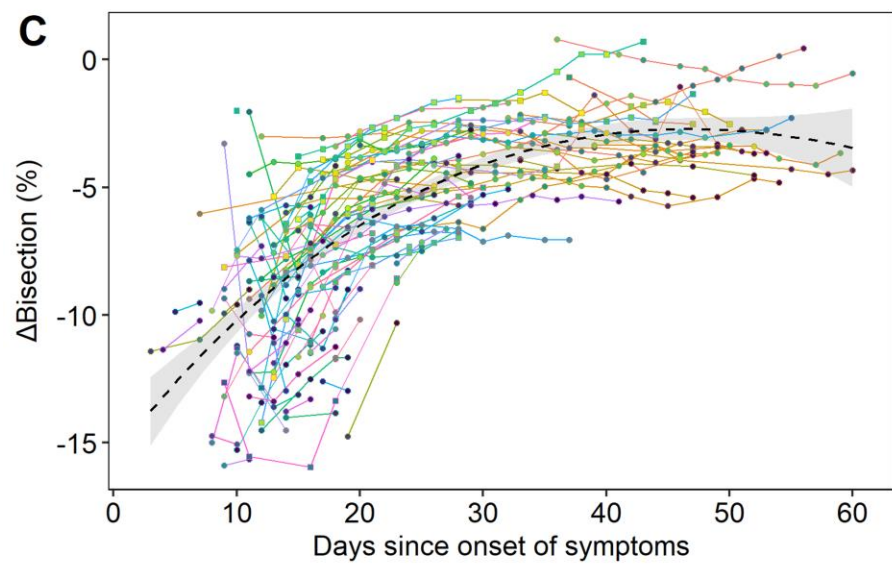
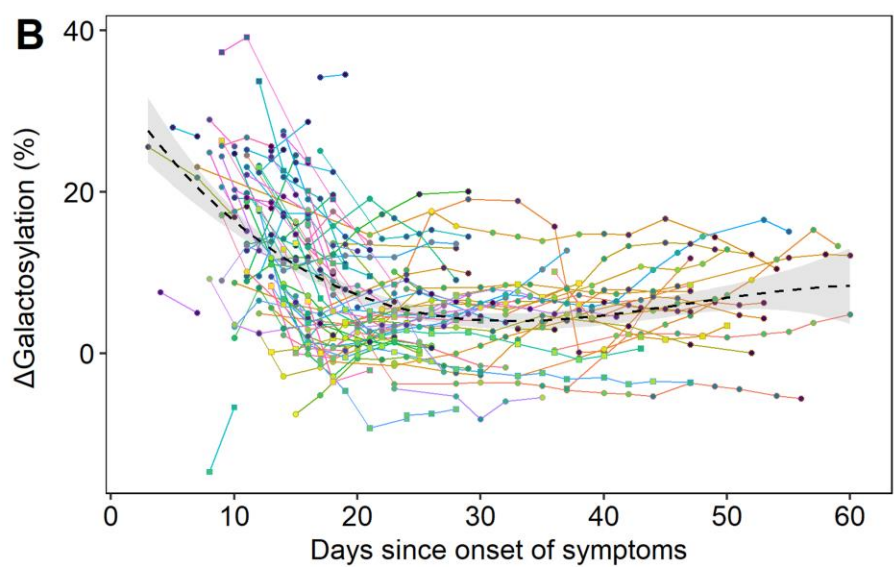
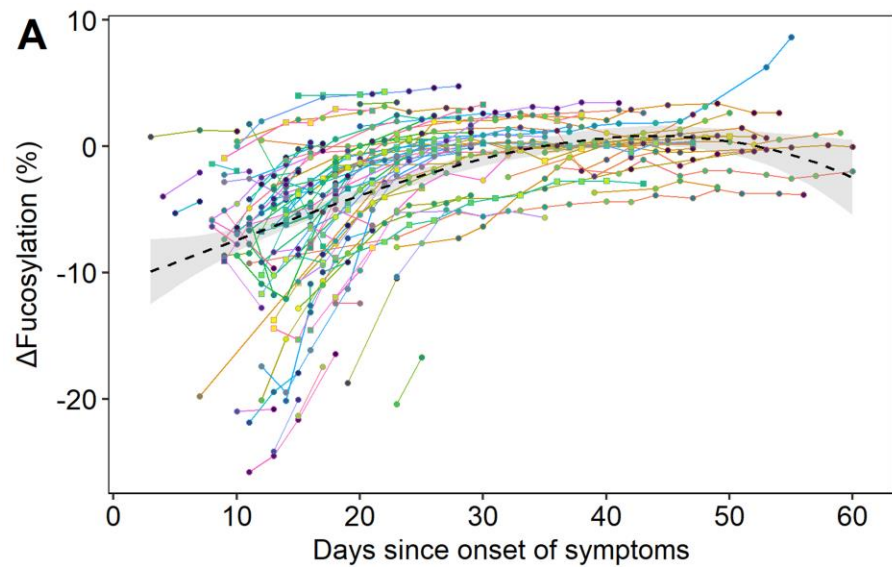
249 The Fc glycosylation signatures of anti-S and total IgG1 were compared pairwise at hospitalization  
250 with regard to fucosylation, bisection, galactosylation and sialylation (**Figure 1, Table S5**).  
251 Fucosylation of anti-S was significantly lower than total (fold change (FC): 0.93;  $p$ -value:  $3.4 \times 10^{-24}$ )  
252 (**Figure 1A, Table S5**). Notably, a prominently low anti-S fucosylation (<85%) was found for 56  
253 patients, with a few patients showing levels as low as 66% (**Figure 1A**). Similarly, bisection of anti-S  
254 was markedly lower than total IgG1 (FC: 0.33;  $p$ -value:  $3.1 \times 10^{-27}$ ) (**Figure 1B**). Anti-S galactosylation  
255 (FC: 1.35;  $p$ -value:  $8.1 \times 10^{-26}$ ) (**Figure 1C**) and sialylation (FC: 1.45;  $p$ -value:  $2.7 \times 10^{-26}$ ) (**Figure 1D**)  
256 were elevated as compared to their total IgG1 counterpart.



257 **Figure 1. Comparison of anti-S (blue) and total (yellow) IgG1 Fc glycosylation.** Relative abundance of IgG1 (A)  
258 fucosylation, (B) bisection, (C) galactosylation and (D) sialylation of anti-S and total IgG1 are given at hospitalization  
259 (n=159). Boxplots display the median and the interquartile range, whereas whiskers represent the first and third quartiles.  
260 A Wilcoxon signed-rank test was used to compare anti-S with total IgG1. \*\*\*\*:  $p$ -value < 0.0001.  
261

### 262 3.2 Dynamic regulation of IgG1 Fc glycosylation in COVID-19

263 Next, we explored the changes of glycosylation over time. Anti-S glycosylation was found to be highly  
264 dynamic, but also total IgG1 glycosylation showed changes in the course of the disease (**Figure S6**).  
265 Both anti-S and total IgG1 galactosylation was found to be confounded by age and sex (**Figure S2**) in  
266 line with literature on IgG Fc glycosylation.<sup>27</sup> Therefore, delta ( $\Delta$ ) values were calculated by  
267 subtracting total from anti-S IgG1 levels to eliminate the confounding effect, and used hereafter  
268 (**Figure S2-3**).



Survival □ Death ○ Discharge

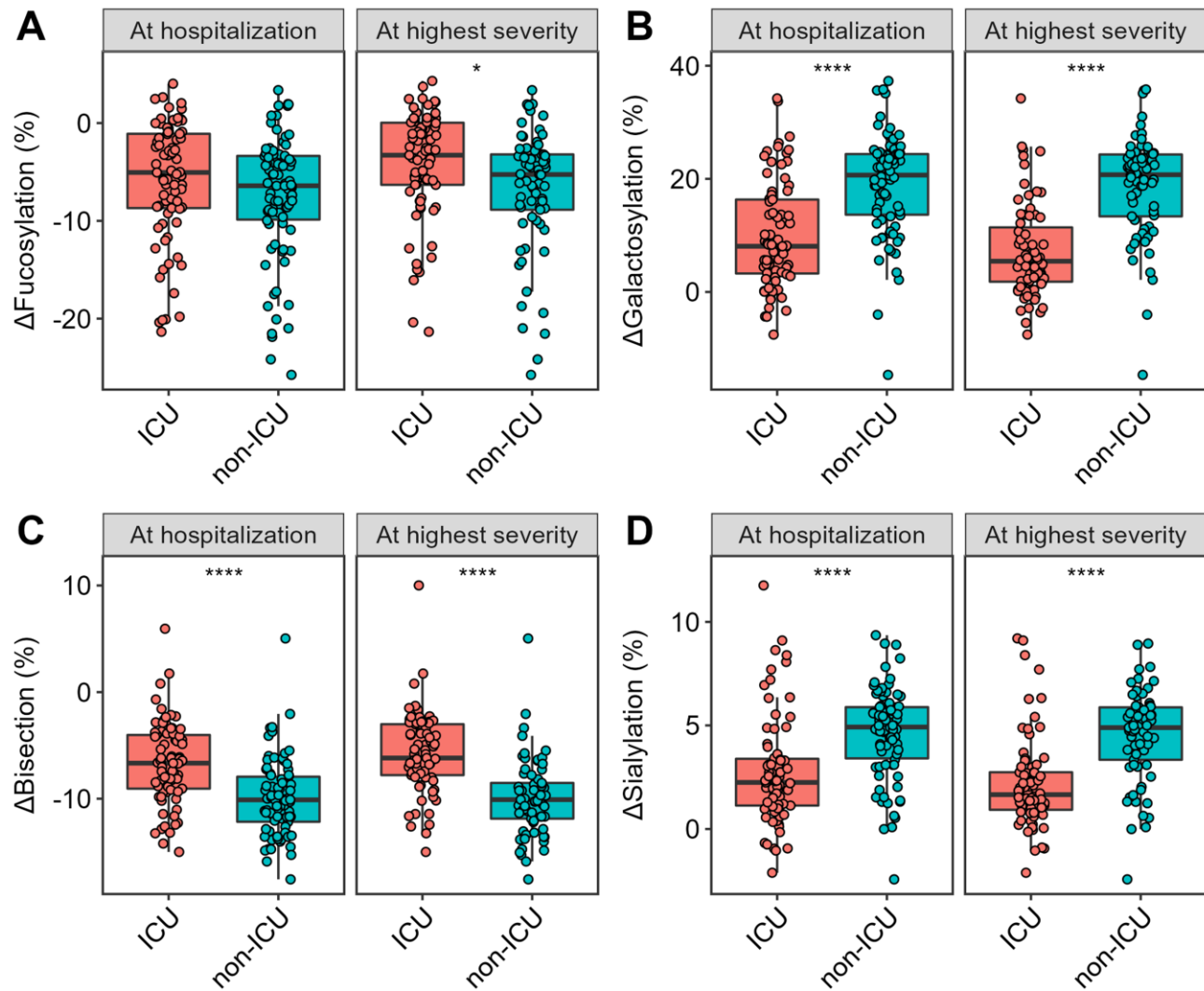


270 **Figure 2.  $\Delta$ Glycosylation dynamics until 60 days since symptom onset.** The time course of  $\Delta$ glycosylation traits (A)  
271 fucosylation, (B) galactosylation, (C) bisection and (D) sialylation as shown during the hospitalization period (n=109). Line  
272 colors correspond to a single COVID-19 patient, whilst the color gradient in the circles/squares indicate the corresponding  
273 severity score (grey = NA). The shape displays whether a patient passed away (square) or was discharged alive (circle).  
274 The black dashed line with a grey 95% confidence interval band is a cubic polynomial fit over the shown datapoints to  
275 illustrate overall dynamics. Late timepoints and two outliers are shown in the **Supplementary Material** due to spatial  
276 constraints (**Figure S4-5**), as well as anti-S and total IgG1 glycosylation dynamics (**Figure S6**).

277 The longitudinal samples allowed us to establish the time course of  $\Delta$ IgG1 glycosylation during  
278 hospitalization, normalized for day of onset of symptoms (**Figure 2, Table S1**). Interestingly, all  
279 glycosylation traits showed a transient pattern for most patients, and were characterized by profound  
280 dynamics, as illustrated by the timelines of individual patients (as indicated by differential line  
281 coloring) and by the fit cubic polynomial line (**Figure 2**). Fucosylation (**Figure 2A**) and bisection  
282 (**Figure 2C**) showed a rapid increase within days and weeks after onset of the disease, followed by a  
283 plateau and approximation of the glycosylation patterns of total IgG1 (**Figure S6**). In contrast,  
284 galactosylation (**Figure 2B**) and sialylation (**Figure 2D**) quickly declined in the first days and weeks,  
285 with the decrease continuing for a long period albeit at lower pace. At the moment of hospital discharge  
286 anti-S galactosylation and sialylation were still slightly higher than total IgG1. Since 19 patients  
287 returned for follow-up sampling after hospital discharge, we noted that for most, fucosylation and  
288 bisection largely remained constant or slightly increased, whilst galactosylation and sialylation  
289 continued to decrease since the last available timepoint (**Figure S5**).

### 290 **3.3 IgG1 Fc glycosylation associates with ICU admission**

291 To investigate whether Fc glycosylation was associated with intensive care unit (ICU) admission,  
292 patients were stratified based on treatment need. This resulted in two groups: 1) patients who at some  
293 point during hospitalization were admitted to the ICU, and 2) patients who were not enrolled to ICU  
294 treatment at all (non-ICU) during hospitalization.  $\Delta$ IgG1 glycosylation derived traits fucosylation,  
295 bisection, galactosylation and sialylation of the above groups were compared both at time of  
296 hospitalization and at the time point of their highest disease severity (**Figure 3, Table S6**).

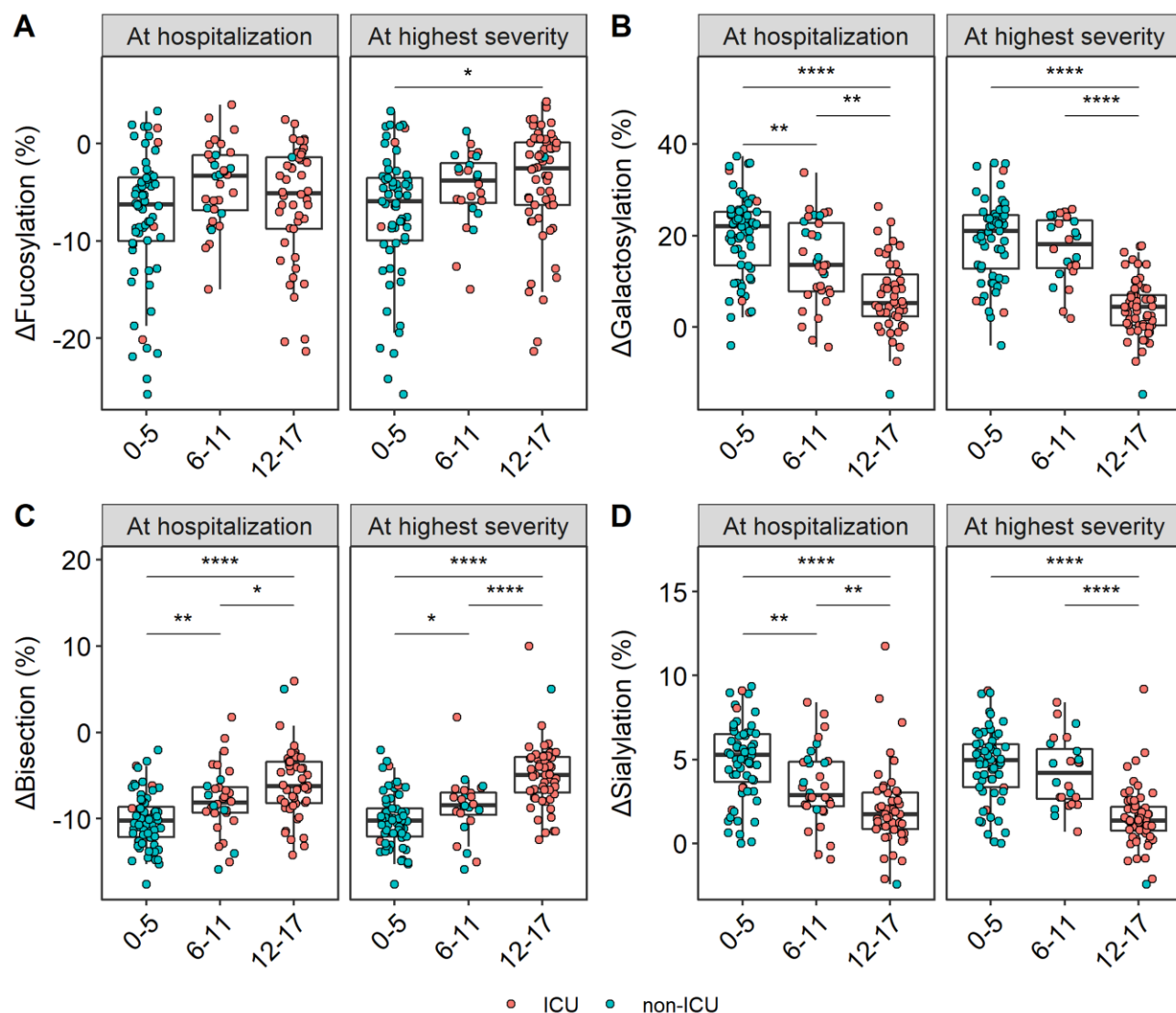


297  
 298 **Figure 3. Comparison of  $\Delta$ glycosylation traits of patients admitted to ICU (red) or non-ICU (blue) treatment.** Shown  
 299 in the facets are the relative levels of  $\Delta$ IgG1 (A) fucosylation, (B) galactosylation, (C) bisection and (D) sialylation at the  
 300 time of hospitalization (left;  $n=159$ ; 77 ICU and 82 non-ICU patients, respectively) and at the time of highest disease  
 301 severity (right;  $n=144$ ; 75 ICU and 69 non-ICU patients, respectively). The highest severity timepoint has been defined for  
 302 each patient as the earliest possible timepoint with highest severity score during hospitalization. A Wilcoxon rank-sum test  
 303 was used to compare ICU and non- ICU patients (Table S6). \*, \*\*\*\*:  $p$ -value < 0.05, 0.0001, respectively. Glycosylation  
 304 dynamics of ICU and non-ICU patients between day 10 and 25 are shown in Figure S8.

305  $\Delta$ IgG1 Fc glycosylation of ICU patients showed a different profile from those of non-ICU patients,  
 306 with the latter being characterized by lower bisection (FC: 0.66,  $p$ -value:  $7.2 \times 10^{-8}$ ) (Figure 3C), and  
 307 higher galactosylation (FC: 0.39,  $p$ -value:  $2.9 \times 10^{-9}$ ) (Figure 3B) and sialylation (FC: 0.46,  $p$ -value:  
 308  $1.7 \times 10^{-7}$ ) at the time of hospitalization (Figure 3D). This difference was maintained or even more  
 309 pronounced at the time of highest disease severity (FC: 0.61, 0.26, 0.34;  $p$ -value:  $1.9 \times 10^{-10}$ ,  $4.1 \times 10^{-12}$ ,  
 310  $3.4 \times 10^{-9}$ , for  $\Delta$ bisection,  $\Delta$ galactosylation and  $\Delta$ sialylation, respectively) (Table S6). Fucosylation  
 311 levels of the ICU group were higher at the time of highest disease severity (FC 0.62;  $p$ -value: 0.012),  
 312 but remained similar at the time of hospital admission (Figure 3A). To confirm that the observed  
 313 effects were not confounded by vast glycosylation dynamics, a subset of non-ICU and ICU patients  
 314 were created and compared, which resulted in comparable observations with regards to  $\Delta$ bisection,  
 315  $\Delta$ galactosylation and  $\Delta$ sialylation as shown above (Figure S7-8).

### 316 3.4 IgG1 Fc glycosylation associates with disease severity

317 Patients were stratified into three groups based on their severity score: 1) severity score between 0-5  
 318 (low severity), 2) 6-11 (intermediate severity) and 3) 12-17 (high severity). Similarly as before,  $\Delta$ IgG1  
 319 glycosylation traits were compared both at time of hospitalization and at time of highest disease  
 320 severity (**Figure 4, Table S7**).



321  
 322 **Figure 4. Comparison of  $\Delta$ glycosylation of patients in different severity score groups.** Shown in the facets are the  
 323 relative levels of  $\Delta$ IgG1 (A) fucosylation, (B) bisection, (C) galactosylation and (D) sialylation at the time of hospitalization  
 324 (left; n=142; 64 low severity, 32 intermediate severity and 46 high severity patients, respectively) and at the time of highest  
 325 disease severity (right; n=144; 61 low severity, 24 intermediate severity and 59 high severity patients, respectively).  
 326 Color indicates ICU (red) and non-ICU (blue) patients. A Wilcoxon rank-sum test was used to compare the different  
 327 severity score groups (**Table S7**). \*, \*\*, \*\*\*\*:  $p$ -value < 0.05, 0.01, 0.0001, respectively.

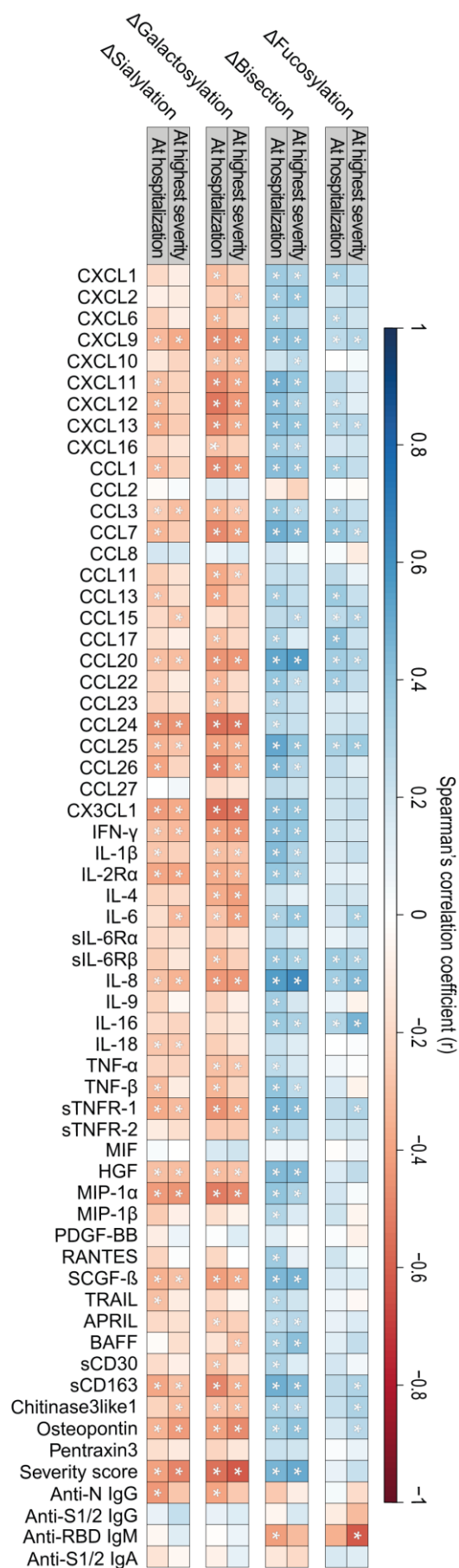
328  $\Delta$ Bisection was found to be increased in groups with increased disease severity (**Figure 4C**), whereas  
 329  $\Delta$ galactosylation (**Figure 4B**) and  $\Delta$ sialylation (**Figure 4D**) patterns were found to be decreased with  
 330 increased disease severity at the time of hospitalization (**Table S7**). These observations were largely  
 331 maintained at highest disease severity (**Figure 4, Table S7**). Higher fucosylation marked the time of  
 332 highest disease severity, but remained rather stable at the time of hospital admission between all groups  
 333 (**Figure 4A, Table S7**). To confirm that the observed effects were not confounded due to profound  
 334 glycosylation dynamics, subsets of patients matched for the time since disease onset were compared,  
 335 which resulted in similar observations with regards to  $\Delta$ galactosylation and  $\Delta$ sialylation as shown

336 above, whereas we could not exclude a potential confounding effect for the bisection signature, maybe  
337 caused by swift glycosylation dynamics, low sample size, or the combination thereof (**Figure S9**).  
338 Apart from ICU admission and severity score, we tested acute respiratory syndrome, ventilation and  
339 survival, and found  $\Delta$ bisection being higher for patients at baseline who passed away later (**Figure**  
340 **S10**).

### 341 **3.5 IgG1 Fc glycosylation associates with inflammatory markers**

342 Multiple inflammatory mediators (in serum) and clinical parameters were measured for patients  
343 enrolled during the first wave of the pandemic. These include members of the CXC, CCL and CX3C  
344 chemokine families, cytokines and corresponding soluble receptors, acute phase proteins and other  
345 mediators involved in the immune response as well as severity scores and anti-viral antibody titers. In  
346 general, negative associations were found between  $\Delta$ galactosylation and  $\Delta$ sialylation and positive  
347 associations for  $\Delta$ bisection and  $\Delta$ fucosylation with inflammatory markers at baseline. One notable  
348 exception was a strong negative correlation between anti-RBD IgM levels and  $\Delta$ bisection and  
349  $\Delta$ fucosylation at baseline and at highest severity, respectively.  $\Delta$ Sialylation associated negatively with  
350 various chemokines, such as CCL24 ( $r = -0.45$ ), CX3CL1 ( $r = -0.43$ ), CCL25 ( $r = -0.34$ ), certain  
351 cytokines, such as IL-8 ( $r = -0.29$ ), IFN- $\gamma$  ( $r = -0.3$ ) and several other variables (**Figure 5, Table S8**).





353 **Figure 5. Heatmap visualizing Spearman's correlations between  $\Delta$ glycosylation traits and inflammatory markers at**  
354 **time of hospitalization (left side of each panel; n=58) and at time of highest disease severity (right side of each panel;**  
355 **n=59). Asterisk (\*) indicates a significant Spearman's correlation ( $p$ -value < 0.05).**

356 Comparable, and largely overlapping negative associations were found for  $\Delta$ galactosylation as for  
357  $\Delta$ sialylation: CCL24 ( $r = -0.55$ ), CX3CL1 ( $r = -0.56$ ), CCL25 ( $r = -0.41$ ), IL-8 ( $r = -0.44$ ), INF- $\gamma$  ( $r =$   
358  $-0.4$ ) and TNF- $\beta$  ( $r = -0.33$ ). Conversely,  $\Delta$ bisection associated positively with IL-8 ( $r = 0.56$ ), CCL25  
359 ( $r = 0.52$ ) and CX3CL1 ( $r = 0.56$ ). Additionally, severity score negatively correlated with  
360  $\Delta$ galactosylation ( $r = -0.55$ ) and  $\Delta$ sialylation ( $r = -0.41$ ) and positively with  $\Delta$ bisection ( $r = 0.46$ ).  
361 Positive associations were found between  $\Delta$ fucosylation and inflammatory markers, including CCL17  
362 ( $r = 0.41$ ) and IL-8 ( $r = 0.34$ ). The above described baseline correlations were comparable to those at  
363 the time of highest disease severity, but a vast body of associations were temporary (**Figure 5, Table**  
364 **S8**).

#### 365 4 Discussion

366 In this study, we analyzed total and anti-S IgG1 Fc glycosylation of 159 COVID-19 patients at different  
367 timepoints during their clinical illness. Although several studies reported on the importance of (anti-S)  
368 IgG1 Fc glycosylation and its association with disease severity in COVID-19<sup>6,13,14,28,29</sup>, this study  
369 involves a large, single center cohort that confirms specific anti-S IgG1 glycosylation features as an  
370 early hallmark of severe COVID-19 in an age- and sex-corrected, time-matched dataset at baseline,  
371 and in the longitudinal dimension.

372 Afucosylated IgG1 B cell responses have recently been described to characterize immune reactions  
373 against membrane-embedded antigens in general, and in particular against viral infections caused by  
374 enveloped viruses such as COVID-19.<sup>13</sup> Foregoing studies showed that severe, hospitalized patients  
375 exhibit a decreased anti-S IgG1 fucosylation as compared to mild, non-hospitalized patients.<sup>6,13,14</sup>  
376 Accordingly, we likewise observed proinflammatory, low-fucosylation signatures on anti-S as  
377 compared to total IgG1, but found no difference in fucosylation comparing hospitalized ICU patients  
378 versus hospitalized non-ICU patients, which is in line with a previous report on anti-SARS-CoV-2  
379 receptor binding domain (anti-RBD) IgG1 fucosylation.<sup>14</sup> Therefore, based on the early existence of  
380 these proinflammatory signatures in some of the patients, we hypothesize that low fucosylation –  
381 potentially even lower before measurable seroconversion, as hypothesized before<sup>13</sup> – on anti-S IgG1  
382 may act as an early inflammatory signal that promotes the development of a more severe disease in  
383 COVID-19 patients, resulting in hospital admission. However, disease severity between hospitalized  
384 patients could not be further distinguished based on anti-S IgG1 fucosylation. Furthermore, hardly any  
385 negative associations were found between anti-S IgG1 fucosylation and inflammatory markers in this  
386 study, unlike in previous reports, where *in vitro* experiments demonstrated that the stimulation of  
387 isolated macrophages with recombinant, glycoengineered anti-S or patient sera-derived low-fucose  
388 IgG1 antibodies trigger higher proinflammatory cytokine release than those with normal fucose  
389 levels.<sup>6,13,14</sup> However, high proinflammatory cytokine levels are not necessarily present in all severe  
390 patients<sup>30</sup>, and this contrasting observation suggests a different regulation and/or the temporal  
391 resolution of fucosylation and cytokine production dynamics *in vivo*. Additionally, beyond or in  
392 combination with low anti-S IgG1 fucosylation a pre-existing risk factor may play a role in COVID-  
393 19 disease severity, which hitherto remained unclear.<sup>29</sup> Of note, the anti-S and anti-RBD IgG1 Fc  
394 glycosylation data were all determined from the circulation, and it is unclear to which extent this would  
395 reflect the inflammatory pattern and glycosylation profile of anti-S antibodies in the lung. Our results  
396 demonstrate that the proinflammatory fucosylation signature that is observed at the early time points  
397 in the disease tends to fade with the course of the disease, which one may interpret as a shift towards a  
398 more anti-inflammatory Fc glycosylation profile that is maintained over time. The absence of core

399 fucose is known to enhance a proinflammatory immune response by activating FcγRIII receptors on  
400 monocytes, macrophages and NK cells.<sup>10</sup> Decreased fucosylation on specific IgG1 has been described  
401 in HIV<sup>13,31</sup> and dengue fever<sup>32</sup>, as well as in alloimmune diseases.<sup>33-37</sup> However, whilst afucosylation  
402 of specific IgG1 plays a protective role in HIV, it clearly marks high disease severity in dengue,  
403 alloimmune diseases or COVID-19.<sup>6,13,14</sup> Furthermore, low total IgG1 fucosylation has been associated  
404 with outcome of pediatric meningococcal sepsis indicating a systemic inflammation due to the potential  
405 accumulation of airway infections during early childhood.<sup>38</sup> Even though the origin of low fucose IgG  
406 responses is seemingly linked to antigen context and affect mostly specific antibodies<sup>13</sup>, the  
407 mechanisms underlying the dynamics of antibody glycosylation remain elusive.

408 Besides afucosylation, a transient, decreased bisection was found on anti-S IgG1. Recent reports  
409 suggest that severe COVID-19 patients present low levels of bisection both on total IgG (Fc and Fab  
410 combined)<sup>29</sup> and anti-S IgG1<sup>13</sup> relative to mild cases. In contrast, no difference was found in anti-RBD  
411 IgG1 bisection between ICU and non-ICU patients in age- and sex-matched patients<sup>14</sup>, albeit these  
412 disease groups were largely comparable to the ones in our study. While bisection associated positively  
413 with ICU admission, disease severity and survival in our study, it lacks functional relevance based on  
414 our current understanding and has no effect on FcγRIII or C1q binding.<sup>10,39</sup>

415 Elevated galactosylation and sialylation of anti-S IgG1 were associated with a less severe disease  
416 course upon hospitalization, and no ICU admission. Similar observations were made in a previous  
417 report, where severe COVID-19 was characterized by lower anti-S IgG1 galactosylation and sialylation  
418 than mild COVID-19.<sup>13</sup> Interestingly, both anti-S and total IgG1 galactosylation and sialylation  
419 decrease by advancing age. As Larsen et al. compared anti-S IgG1 galactosylation and sialylation of  
420 imperfectly age matched patient groups without age correction, the disease and age effects remained  
421 indiscernible.<sup>13</sup> We describe decreased anti-S IgG1 galactosylation in ICU patients as compared to  
422 non-ICU patients, and analogously, markedly lower specific IgG1 galactosylation has been shown to  
423 characterize the more severe, active phase of tuberculosis as compared to its latent counterpart.<sup>40</sup> Even  
424 though more and more reports support that elevated levels of galactosylated IgG are associated with  
425 the activation of the classical complement pathway<sup>10,12,41</sup>, galactosylation was associated with  
426 increased disease severity in this study, possibly due to the fact that complement can contribute to the  
427 increased inflammation both directly, and through inducing a chemotactic response through C5a,  
428 thereby increasing cellular infiltration to inflamed tissues such as the lung.<sup>42</sup> Elevated sialylation levels  
429 on anti-S IgG1 were associated with increased disease severity in the current report. Sialylation has  
430 been broadly described as critical in mediating anti-inflammatory activity<sup>43-45</sup>, yet it remains to be  
431 elucidated whether sialylated IgG exerts an anti-inflammatory effect in COVID-19.

## 432 **5 Conclusions**

433 This study established anti-S IgG1 bisection, galactosylation and sialylation as a unique combination  
434 of features that associate with ICU admission and disease severity in hospitalized COVID-19 patients.  
435 These features were additionally associated with markers of inflammation. Hence, we believe anti-S  
436 IgG1 glycosylation may be applicable for patient stratification upon hospitalization. The glycosylation  
437 profiles are highly dynamic, the drivers of which remain elusive and to be investigated in future studies.

## 438 **6 Contributors**

439 T. P.: Data (pre)processing, data curation, formal analysis, validation, investigation, visualization,  
440 statistical analysis, data interpretation, conceptualization, writing – original draft preparation. J. N.:  
441 sample preparation, data acquisition (IgG Fc glycosylation), W. W.: sample preparation (IgG Fc

442 glycosylation), F. L.: production and purification of recombinant spike protein, K. E. van M, S. A. J.,  
443 T. H. M. O: data acquisition (soluble marker profiles), review J. J. C. V.: data acquisition (antibody  
444 titers), writing – review & editing, A. H. E. R., S. M. A.: set up of cohort, recruitment & sampling of  
445 participants, writing – review & editing, G.V., C. H. H.: writing – reviewing & editing M. W.:  
446 Supervision, writing – review & editing, conceptualization, funding acquisition.

447 All authors were involved in the critical revision of the manuscript and have given approval to the final  
448 version of the manuscript.

## 449 **7 Declaration of interests**

450 A. H. E. R received support from Crowdfunding Wake Up To Corona, organized by the Leiden  
451 University Fund, participated in grants or contracts with Diorapthe, Stichting apothekers and UNeedle,  
452 participated on a Data Safety Monitoring/Advisory Board of a multicenter Dutch clinical trial (Clinical  
453 trial (RCT) on convalescent plasma for treatment of immunocompromised patients with COVID-19)  
454 and has recently been appointed as member of the EMA scientific advisory group on vaccines (unpaid).

455 The other authors declare that the research was conducted in the absence of any commercial or financial  
456 relationships that could be construed as a potential conflict of interest.

## 457 **8 Funding**

458 This project received funding from the European Commission’s Horizon2020 research and innovation  
459 program for H2020-MSCA-ITN IMforFUTURE, under grant agreement number 721815, and  
460 supported by Crowdfunding Wake Up To Corona, organized by the Leiden University Fund.

## 461 **9 Data sharing**

462 The datasets generated for this study are available on request from the corresponding author.

## 463 **10 References**

- 464 1. Zhou P, Yang XL, Wang XG, et al. A pneumonia outbreak associated with a new coronavirus  
465 of probable bat origin. *Nature* 2020; **579**(7798): 270-3.
- 466 2. Dong E, Du H, Gardner L. An interactive web-based dashboard to track COVID-19 in real  
467 time. *The Lancet Infectious Diseases* 2020; **20**(5): 533-4.
- 468 3. Oran DP, Topol EJ. Prevalence of Asymptomatic SARS-CoV-2 Infection : A Narrative  
469 Review. *Ann Intern Med* 2020; **173**(5): 362-7.
- 470 4. Long QX, Liu BZ, Deng HJ, et al. Antibody responses to SARS-CoV-2 in patients with  
471 COVID-19. *Nat Med* 2020; **26**(6): 845-8.
- 472 5. Hu B, Guo H, Zhou P, Shi ZL. Characteristics of SARS-CoV-2 and COVID-19. *Nat Rev*  
473 *Microbiol* 2021; **19**(3): 141-54.
- 474 6. Hoepel W, Chen HJ, Geyer CE, et al. High titers and low fucosylation of early human anti-  
475 SARS-CoV-2 IgG promote inflammation by alveolar macrophages. *Sci Transl Med* 2021; **13**(596).
- 476 7. Ankerhold J, Giese S, Kolb P, et al. Circulating multimeric immune complexes drive  
477 immunopathology in COVID-19. *bioRxiv* 2021.



- 478 8. Bruhns P, Jonsson F. Mouse and human FcR effector functions. *Immunol Rev* 2015; **268**(1):  
479 25-51.
- 480 9. Lauc G, Pezer M, Rudan I, Campbell H. Mechanisms of disease: The human N-glycome.  
481 *Biochim Biophys Acta* 2016; **1860**(8): 1574-82.
- 482 10. Dekkers G, Treffers L, Plomp R, et al. Decoding the Human Immunoglobulin G-Glycan  
483 Repertoire Reveals a Spectrum of Fc-Receptor- and Complement-Mediated-Effector Activities. *Front*  
484 *Immunol* 2017; **8**: 877.
- 485 11. Ferrara C, Grau S, Jager C, et al. Unique carbohydrate-carbohydrate interactions are required  
486 for high affinity binding between Fcγ<sub>3</sub> and antibodies lacking core fucose. *Proc Natl Acad*  
487 *Sci U S A* 2011; **108**(31): 12669-74.
- 488 12. van Osch TLJ, Nouta J, Derksen NIL, et al. Fc Galactosylation Promotes Hexamerization of  
489 Human IgG1, Leading to Enhanced Classical Complement Activation. *J Immunol* 2021; **207**(6): 1545-  
490 54.
- 491 13. Larsen MD, de Graaf EL, Sonneveld ME, et al. Afucosylated IgG characterizes enveloped viral  
492 responses and correlates with COVID-19 severity. *Science* 2021; **371**(6532).
- 493 14. Chakraborty S, Gonzalez J, Edwards K, et al. Proinflammatory IgG Fc structures in patients  
494 with severe COVID-19. *Nat Immunol* 2021; **22**(1): 67-73.
- 495 15. Brouwer PJM, Caniels TG, van der Straten K, et al. Potent neutralizing antibodies from  
496 COVID-19 patients define multiple targets of vulnerability. *Science* 2020; **369**(6504): 643-50.
- 497 16. Falck D, Jansen BC, de Haan N, Wuhler M. High-Throughput Analysis of IgG Fc  
498 Glycopeptides by LC-MS. *Methods Mol Biol* 2017; **1503**: 31-47.
- 499 17. Jansen BC, Falck D, de Haan N, et al. LaCyTools: A Targeted Liquid Chromatography-Mass  
500 Spectrometry Data Processing Package for Relative Quantitation of Glycopeptides. *J Proteome Res*  
501 2016; **15**(7): 2198-210.
- 502 18. Pucic M, Knezevic A, Vidic J, et al. High throughput isolation and glycosylation analysis of  
503 IgG-variability and heritability of the IgG glycome in three isolated human populations. *Mol Cell*  
504 *Proteomics* 2011; **10**(10): M111 010090.
- 505 19. Clerc F, Reiding KR, Jansen BC, Kammeijer GS, Bondt A, Wuhler M. Human plasma protein  
506 N-glycosylation. *Glycoconj J* 2016; **33**(3): 309-43.
- 507 20. van Meijgaarden KE, Khatri B, Smith SG, et al. Cross-laboratory evaluation of multiplex bead  
508 assays including independent common reference standards for immunological monitoring of  
509 observational and interventional human studies. *PLoS One* 2018; **13**(9): e0201205.
- 510 21. Escribano P, Alvarez-Uria A, Alonso R, et al. Detection of SARS-CoV-2 antibodies is  
511 insufficient for the diagnosis of active or cured COVID-19. *Sci Rep* 2020; **10**(1): 19893.
- 512 22. Maine GN, Lao KM, Krishnan SM, et al. Longitudinal characterization of the IgM and IgG  
513 humoral response in symptomatic COVID-19 patients using the Abbott Architect. *Journal of Clinical*  
514 *Virology* 2020; **133**.
- 515 23. Zlei M, Sidorov IA, Joosten S, et al. Absence of rapid T cell control corresponds with delayed  
516 viral clearance in hospitalised COVID-19 patients. *ResearchSquare* 2021.
- 517 24. Zhao J, Yuan Q, Wang H, et al. Antibody Responses to SARS-CoV-2 in Patients With Novel  
518 Coronavirus Disease 2019. *Clin Infect Dis* 2020; **71**(16): 2027-34.

- 519 25. Beavis KG, Matushek SM, Abeleda APF, et al. Evaluation of the EUROIMMUN Anti-SARS-  
520 CoV-2 ELISA Assay for detection of IgA and IgG antibodies. *J Clin Virol* 2020; **129**: 104468.
- 521 26. Knight SR, Ho A, Pius R, et al. Risk stratification of patients admitted to hospital with covid-  
522 19 using the ISARIC WHO Clinical Characterisation Protocol: development and validation of the 4C  
523 Mortality Score. *BMJ* 2020; **370**: m3339.
- 524 27. Kristic J, Vuckovic F, Menni C, et al. Glycans are a novel biomarker of chronological and  
525 biological ages. *J Gerontol A Biol Sci Med Sci* 2014; **69**(7): 779-89.
- 526 28. Bye AP, Hoepel W, Mitchell JL, et al. Aberrant glycosylation of anti-SARS-CoV-2 IgG is a  
527 pro-thrombotic stimulus for platelets. *Blood* 2021; **138**(16): 1481-9.
- 528 29. Petrovic T, Alves I, Bugada D, et al. Composition of the immunoglobulin G glycome associates  
529 with the severity of COVID-19. *Glycobiology* 2021; **31**(4): 372-7.
- 530 30. Kox M, Waalders NJB, Kooistra EJ, Gerretsen J, Pickkers P. Cytokine Levels in Critically Ill  
531 Patients With COVID-19 and Other Conditions. *JAMA* 2020; **324**(15): 1565-7.
- 532 31. Ackerman ME, Crispin M, Yu X, et al. Natural variation in Fc glycosylation of HIV-specific  
533 antibodies impacts antiviral activity. *J Clin Invest* 2013; **123**(5): 2183-92.
- 534 32. Wang TT, Sewatanon J, Memoli MJ, et al. IgG antibodies to dengue enhanced for  
535 Fcγ3 binding determine disease severity. *Science* 2017; **355**(6323): 395-8.
- 536 33. Kapur R, Della Valle L, Sonneveld M, et al. Low anti-RhD IgG-Fc-fucosylation in pregnancy:  
537 a new variable predicting severity in haemolytic disease of the fetus and newborn. *Br J Haematol* 2014;  
538 **166**(6): 936-45.
- 539 34. Kapur R, Kustiawan I, Vestrheim A, et al. A prominent lack of IgG1-Fc fucosylation of platelet  
540 alloantibodies in pregnancy. *Blood* 2014; **123**(4): 471-80.
- 541 35. Sonneveld ME, de Haas M, Koeleman C, et al. Patients with IgG1-anti-red blood cell  
542 autoantibodies show aberrant Fc-glycosylation. *Sci Rep* 2017; **7**(1): 8187.
- 543 36. Sonneveld ME, Koelewijn J, de Haas M, et al. Antigen specificity determines anti-red blood  
544 cell IgG-Fc alloantibody glycosylation and thereby severity of haemolytic disease of the fetus and  
545 newborn. *Br J Haematol* 2017; **176**(4): 651-60.
- 546 37. Sonneveld ME, Natunen S, Sainio S, et al. Glycosylation pattern of anti-platelet IgG is stable  
547 during pregnancy and predicts clinical outcome in alloimmune thrombocytopenia. *Br J Haematol*  
548 2016; **174**(2): 310-20.
- 549 38. de Haan N, Boeddha NP, Ekinci E, et al. Differences in IgG Fc Glycosylation Are Associated  
550 with Outcome of Pediatric Meningococcal Sepsis. *mBio* 2018; **9**(3).
- 551 39. Thomann M, Schlothauer T, Dashivets T, et al. In vitro glycoengineering of IgG1 and its effect  
552 on Fc receptor binding and ADCC activity. *PLoS One* 2015; **10**(8): e0134949.
- 553 40. Lu LL, Das J, Grace PS, Fortune SM, Restrepo BI, Alter G. Antibody Fc Glycosylation  
554 Discriminates Between Latent and Active Tuberculosis. *J Infect Dis* 2020; **222**(12): 2093-102.
- 555 41. Peschke B, Keller CW, Weber P, Quast I, Lunemann JD. Fc-Galactosylation of Human  
556 Immunoglobulin Gamma Isotypes Improves C1q Binding and Enhances Complement-Dependent  
557 Cytotoxicity. *Front Immunol* 2017; **8**: 646.
- 558 42. Carvelli J, Demaria O, Vely F, et al. Association of COVID-19 inflammation with activation  
559 of the C5a-C5aR1 axis. *Nature* 2020; **588**(7836): 146-50.

- 560 43. Kaneko Y, Nimmerjahn F, Ravetch JV. Anti-inflammatory activity of immunoglobulin G  
561 resulting from Fc sialylation. *Science* 2006; **313**(5787): 670-3.
- 562 44. Washburn N, Schwab I, Ortiz D, et al. Controlled tetra-Fc sialylation of IVIg results in a drug  
563 candidate with consistent enhanced anti-inflammatory activity. *Proc Natl Acad Sci U S A* 2015;  
564 **112**(31): E4339.
- 565 45. Quast I, Keller CW, Maurer MA, et al. Sialylation of IgG Fc domain impairs complement-  
566 dependent cytotoxicity. *J Clin Invest* 2015; **125**(11): 4160-70.
- 567

## SUPPORTING INFORMATION

*medRxiv*

### Immunoglobulin G1 Fc glycosylation as an early hallmark of severe COVID-19

Tamas Pongracz<sup>1,\*</sup>, Jan Nouta<sup>1</sup>, Wenjun Wang<sup>1</sup>, Krista. E. van Meijgaarden<sup>4</sup>, Federica Linty<sup>2,3</sup>, Gestur Vidarsson<sup>2,3</sup>, Simone A. Joosten<sup>4</sup>, Tom H. M. Ottenhoff<sup>4</sup>, Cornelis H. Hokke<sup>5</sup>, Jutte J. C. de Vries<sup>6</sup>, Sesmu M. Arbous<sup>7</sup>, Anna H. E. Roukens<sup>7</sup>, Manfred Wuhrer<sup>1</sup> in collaboration with BEAT-COVID<sup>#</sup> and COVID-19<sup>&</sup> groups

<sup>1</sup>Center for Proteomics and Metabolomics, Leiden University Medical Center, Leiden, Netherlands

<sup>2</sup>Dept. of Experimental Immunohematology, Sanquin Research, Amsterdam, Netherlands

<sup>3</sup>Landsteiner Laboratory, Amsterdam University Medical Center, Amsterdam, Netherlands

<sup>4</sup>Dept. of Infectious Diseases, Leiden University Medical Center, Leiden, Netherlands

<sup>5</sup>Dept. of Parasitology, Leiden University Medical Center, Leiden, Netherlands

<sup>6</sup>Dept. of Medical Microbiology, Leiden University Medical Center, Leiden, Netherlands

<sup>7</sup>Dept. of Intensive Care, Leiden University Medical Center, Leiden, Netherlands

**#BEAT-COVID group** (in alphabetical order, investigators): B. M. van den Berg<sup>2</sup>, S. Cannegieter<sup>3</sup>, C. M. Cobbaert<sup>4</sup>, A. van der Does<sup>5</sup>, J. J. M. van Dongen<sup>6</sup>, H. C. J. Eikenboom<sup>7</sup>, M. C. M. Feltkamp<sup>8</sup>, A. Geluk<sup>9</sup>, J. J. Goeman<sup>10</sup>, M. Giera<sup>11</sup>, T. Hankemeier<sup>12</sup>, M. H. M. Heemskerk<sup>13</sup>, P. S. Hiemstra<sup>5</sup>, J. J. Janse<sup>14</sup>, S. P. Jochems<sup>14</sup>, M. Kikkert<sup>8</sup>, L. Lamont<sup>12</sup>, J. Manniën<sup>10</sup>, M. R. del Prado<sup>1</sup>, N. Queralt Rosinach<sup>15</sup>, M. Roestenberg<sup>14</sup>, M. Roos<sup>15</sup>, H. H. Smits<sup>14</sup>, E. J. Snijder<sup>8</sup>, F. J. T. Staal<sup>6</sup>, L. A. Trouw<sup>6</sup>, R. Tsonaka<sup>10</sup>, A. Verhoeven<sup>11</sup>, L. G. Visser<sup>9</sup>, J. J. C. de Vries<sup>8</sup>, D. J. van Westerloo<sup>1</sup>, J. Wigbers<sup>1</sup>, H. J. van der Wijk<sup>10</sup>, R. C. van Wissen<sup>4</sup>, M. Yazdanbakhsh<sup>14</sup>, M. Zlei<sup>6</sup>

<sup>1</sup>Dept. of Intensive Care, Leiden University Medical Center, Leiden, Netherlands

<sup>2</sup>Dept. of Internal Medicine, Nephrology, Leiden University Medical Center, Leiden, Netherlands

<sup>2</sup>Dept. of Clinical Epidemiology, Leiden University Medical Center, Leiden, Netherlands

<sup>4</sup>Dept. of Clinical Chemistry, Leiden University Medical Center, Leiden, Netherlands

<sup>5</sup>Dept. of Pulmonary Medicine, Leiden University Medical Center, Leiden, Netherlands

<sup>6</sup>Dept. of Immunology, Leiden University Medical Center, Leiden, Netherlands

<sup>7</sup>Dept. of Internal Medicine, Thrombosis and Hemostasis, Leiden University Medical Center, Leiden, Netherlands

<sup>8</sup>Dept. of Medical Microbiology, Leiden University Medical Center, Leiden, Netherlands

<sup>9</sup>Dept. of Infectious Diseases, Leiden University Medical Center, Leiden, Netherlands

<sup>10</sup>Dept. of Biomedical Data Sciences, Leiden University Medical Center, Leiden, Netherlands

<sup>11</sup>Center for Proteomics and Metabolomics, Leiden University Medical Center, Leiden, Netherlands

<sup>12</sup>Dept. of Analytical Biosciences, Leiden Academic Centre for Drug Research, Leiden, Netherlands

<sup>13</sup>Dept. of Hematology, Leiden University Medical Center, Leiden, Netherlands

<sup>14</sup>Dept. of Parasitology, Leiden University Medical Center, Leiden, Netherlands

<sup>15</sup>Dept. of Human Genetics, Leiden University Medical Center, Leiden, Netherlands

**&COVID-19 group** (in alphabetical order, investigators):

M. Baysan<sup>2,3</sup>, M. G. J. de Boer<sup>4</sup>, A. G. van der Bom<sup>3</sup>, O. M. Dekkers<sup>3</sup>, A. M. Eikenboom<sup>3</sup>, S. B. ter Haar<sup>3</sup>, L. Heerdink<sup>3</sup>, L. J. van Heurn<sup>3</sup>, I. de Jonge<sup>3</sup>, W. Lijfering<sup>3</sup>, R. Meier<sup>1</sup>, J. A. Oud<sup>1</sup>, F. Rosendaal<sup>3</sup>, A. G. L. Toppenberg<sup>3</sup>, J. Uzorka<sup>4</sup>, A. A. van IJzinga Veenstra, J. Wigbers<sup>2</sup>, J. M. Wubboldts<sup>4</sup>

<sup>1</sup>Dept. of Hematology, Leiden University Medical Center, Leiden, Netherlands

<sup>2</sup>Dept. of Intensive Care, Leiden University Medical Center, Leiden, Netherlands

<sup>3</sup>Dept. of Clinical Epidemiology, Leiden University Medical Center, Leiden, Netherlands

<sup>4</sup>Dept. of Infectious Diseases, Leiden University Medical Center, Leiden, Netherlands

**\*Correspondence:**

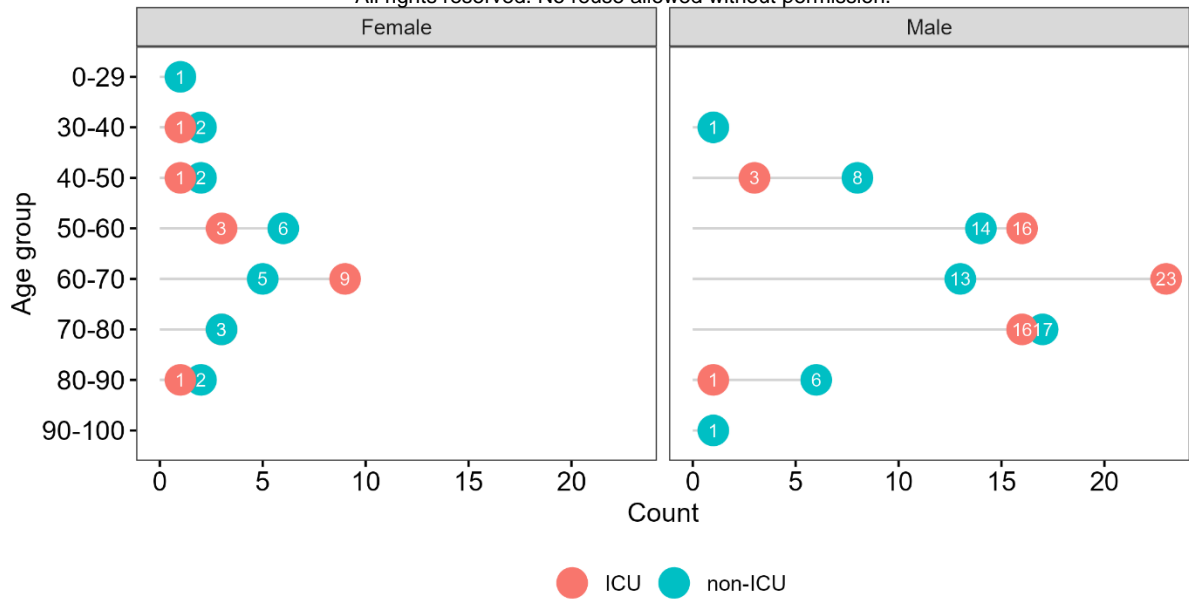
Tamas Pongracz

Albinusdreef 2, 2223ZA, Leiden, Netherlands

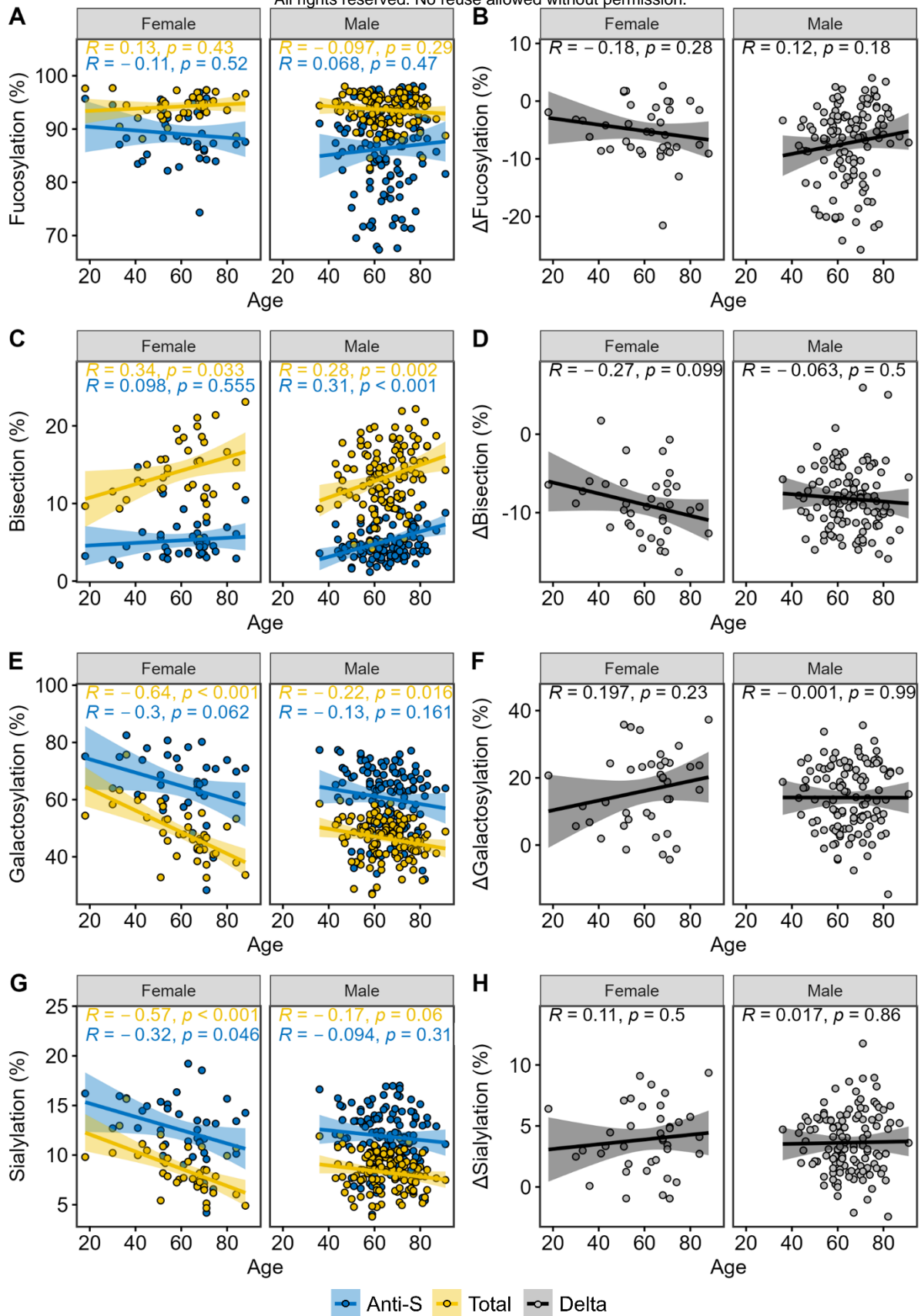
Tel: +31 71 526 8701

[t.pongracz@lumc.nl](mailto:t.pongracz@lumc.nl)



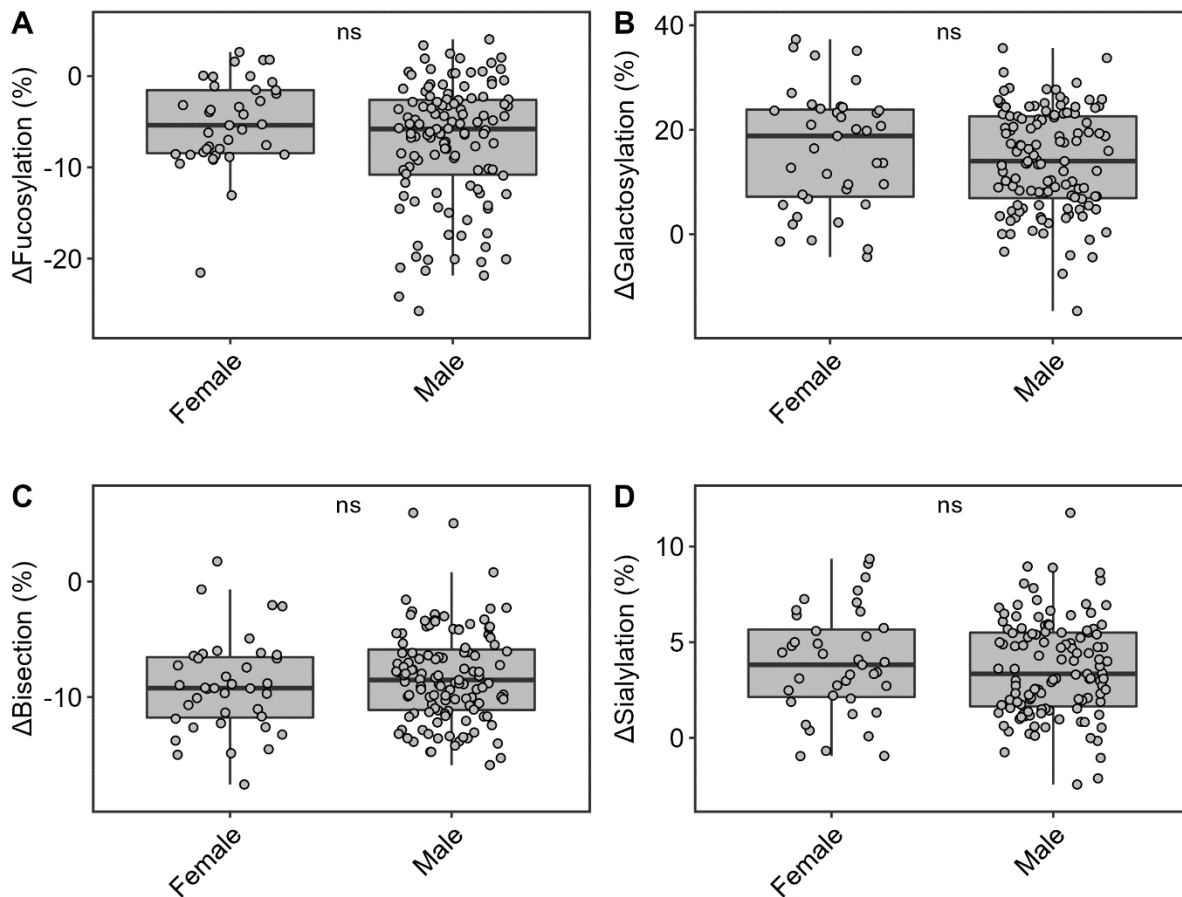


**Supplementary Figure 1. Age and sex distribution in the BEAT-COVID cohort.** Overall 159 patients participated in the study (39 female and 119 male, 1 unknown (not shown)). The color illustrates ICU (red) and non-ICU (blue) treatment groups, whereas the number in the circles indicates the number of patients in the corresponding group.

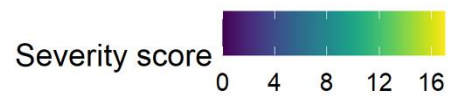
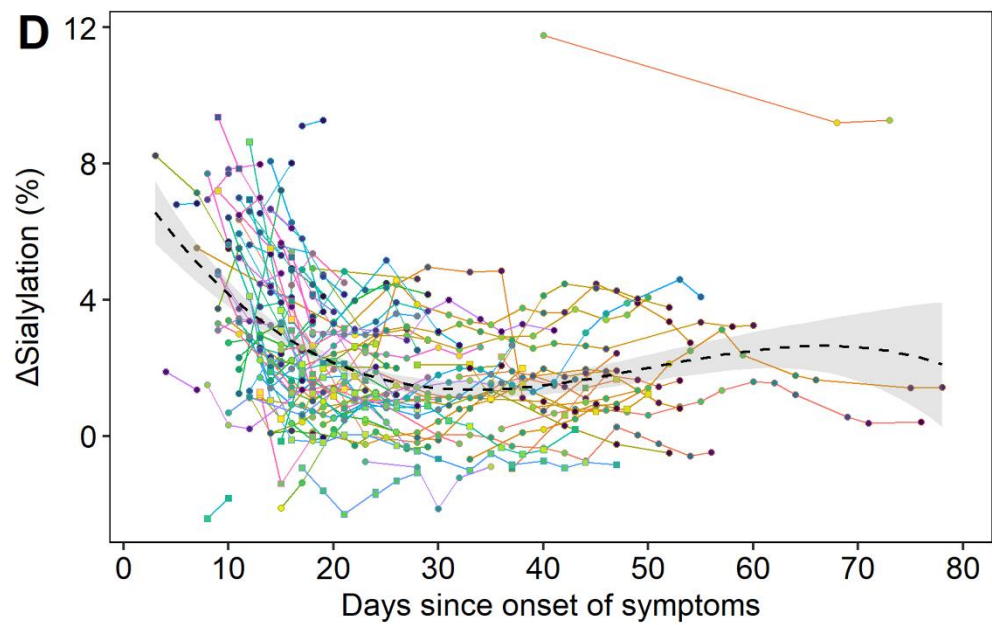
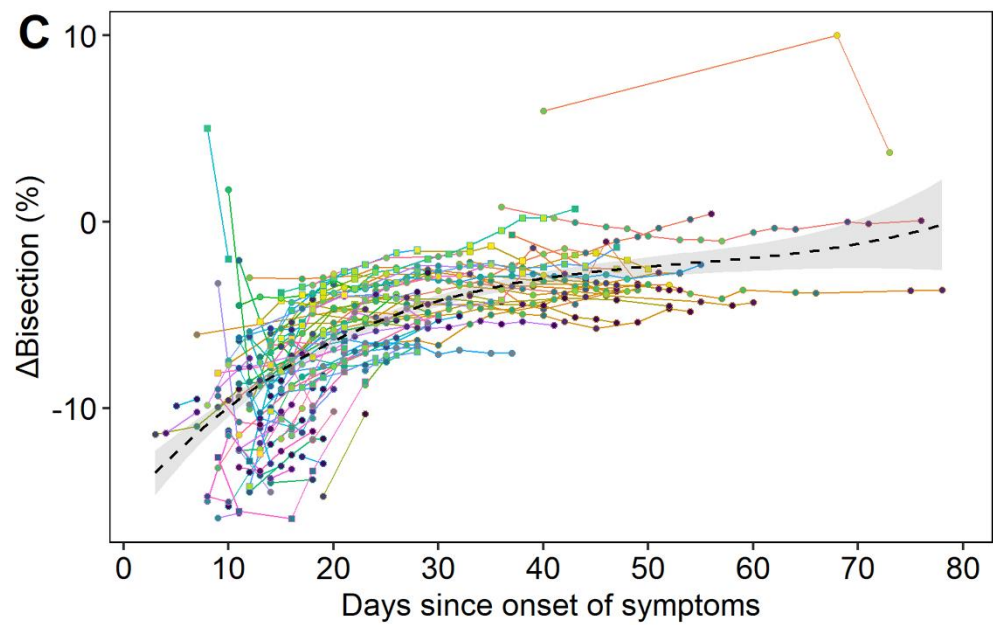
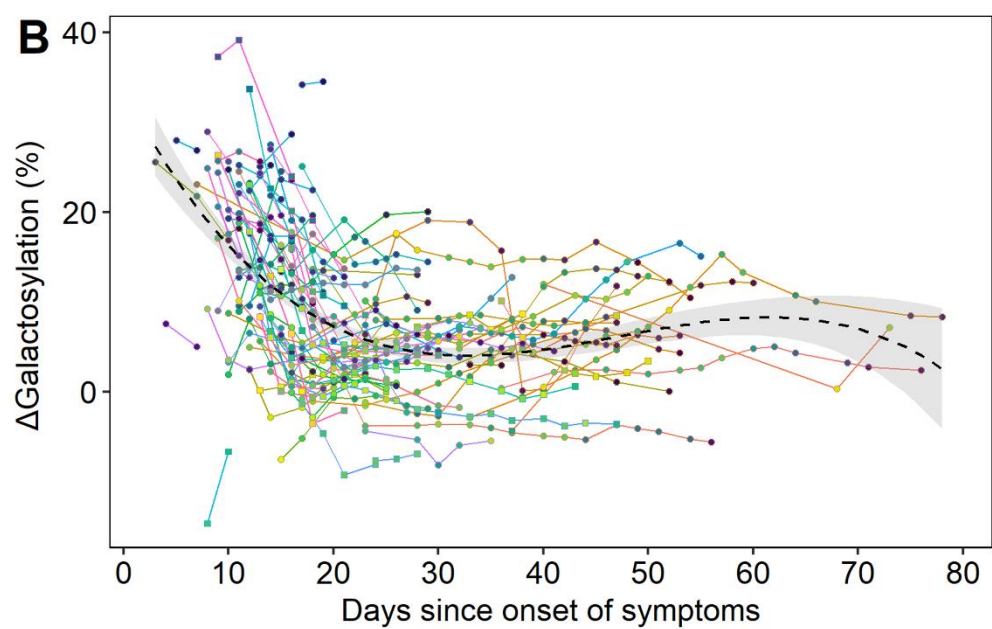
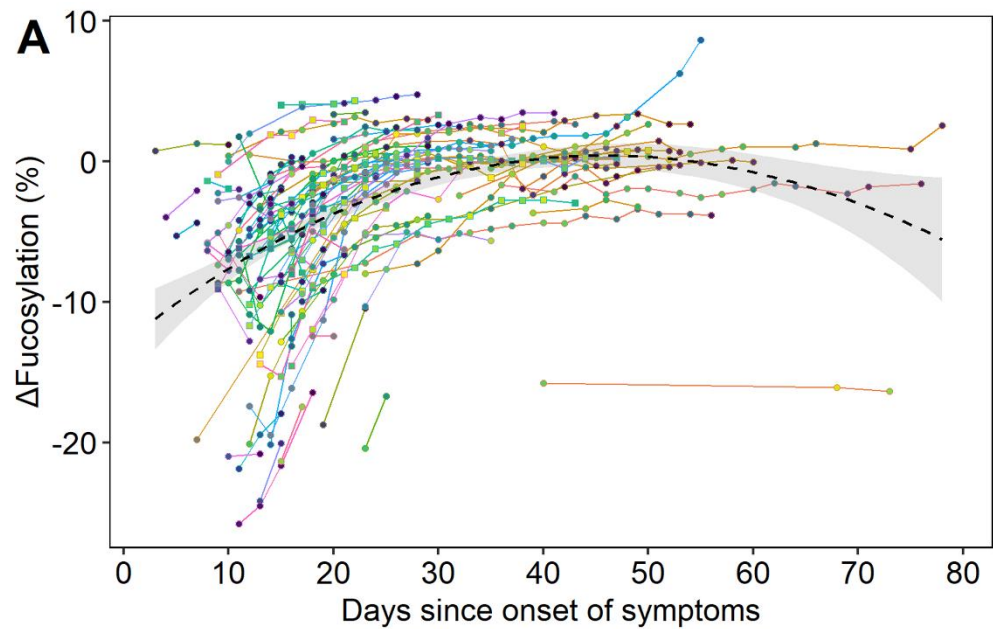


**Supplementary Figure 2. Anti-S (blue) and total (yellow) IgG1 bisection, galactosylation and sialylation are confounded by age in a similar way, which is eliminated by normalizing to total IgG1 levels. IgG1 (A) fucosylation, (C) bisection, (E) galactosylation and (G) sialylation as a proxy of age in female (left) and male (right) patients. Corresponding delta ( $\Delta$ ) IgG1 (B) fucosylation and (D) bisection, (F) galactosylation and (H)**

All rights reserved. No reuse allowed without permission.  
sialylation levels (all in grey), as normalized to total IgG levels by subtracting total from anti-S IgG1 glycosylation levels. Baseline timepoints are shown. Shown in the inset are the Spearman correlation coefficients ( $R$ ) and  $p$ -values, respectively. IgG1 bisection is known to increase, whereas galactosylation and sialylation are known to decrease upon aging.<sup>1</sup> Correction for the age confounding effect was performed by normalizing to total IgG levels, as illustrated by the weak and non-significant Spearman correlations and  $p$ -values, respectively (**B**, **D**, **F**, **H**).



**Supplementary Figure 3. Comparison of  $\Delta$ glycosylation traits of female and male patients demonstrates the absence of a sex confounding effect. IgG1 (A)  $\Delta$ fucosylation, (B)  $\Delta$ galactosylation, (C)  $\Delta$ bisection and (D)  $\Delta$ sialylation. Correction for the age and sex confounding effect was performed as described above (Figure S2).**

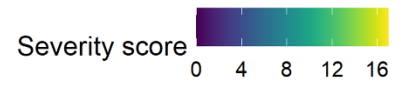
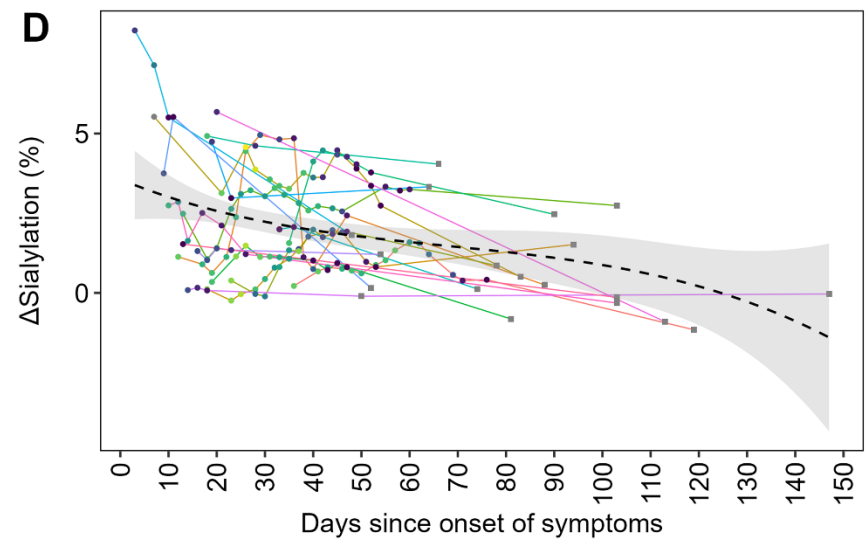
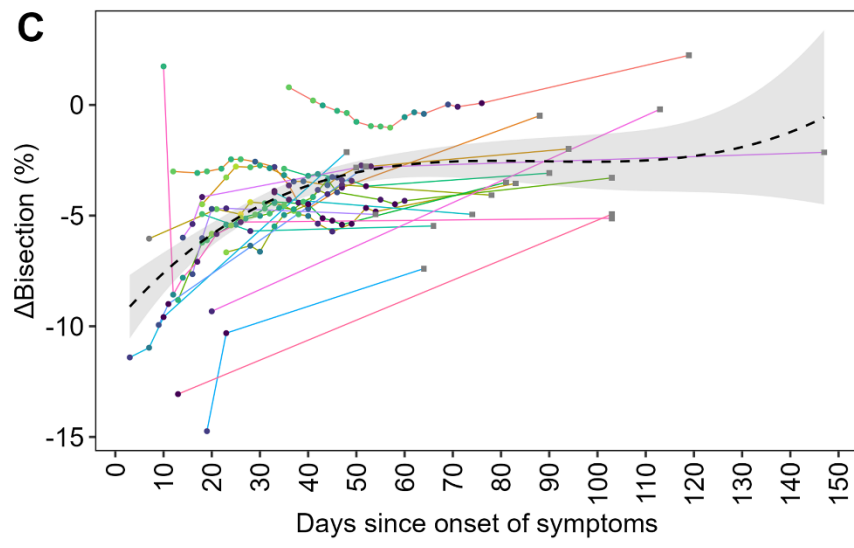
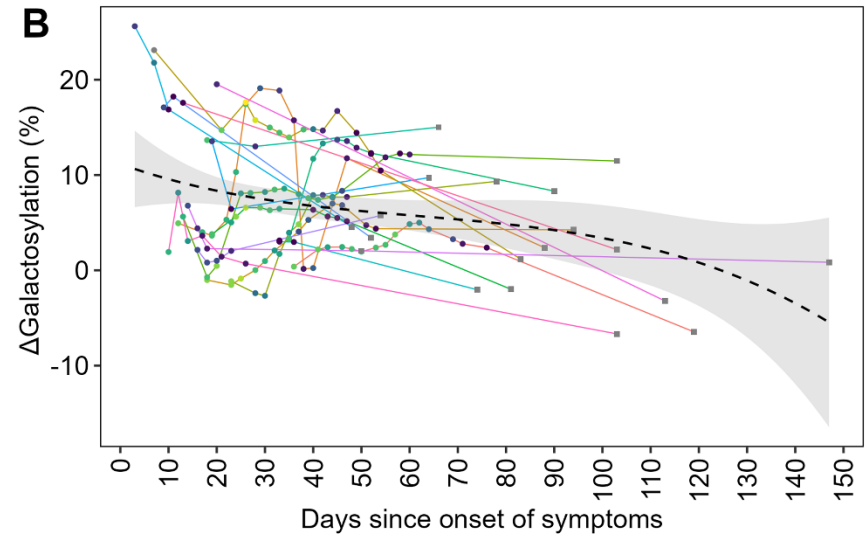
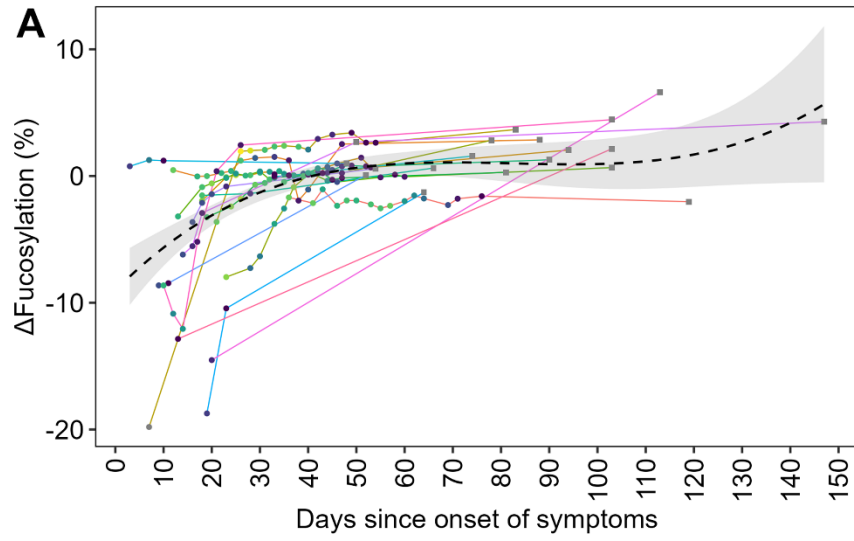


Survival □ Death ○ Discharge

All rights reserved. No reuse allowed without permission.

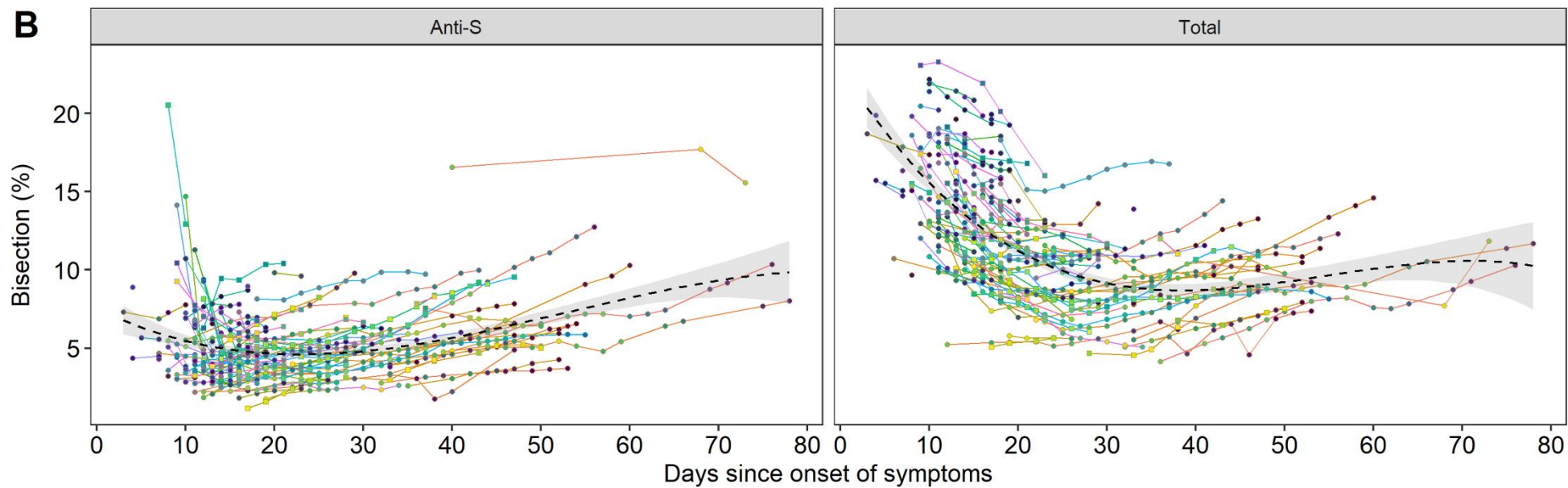
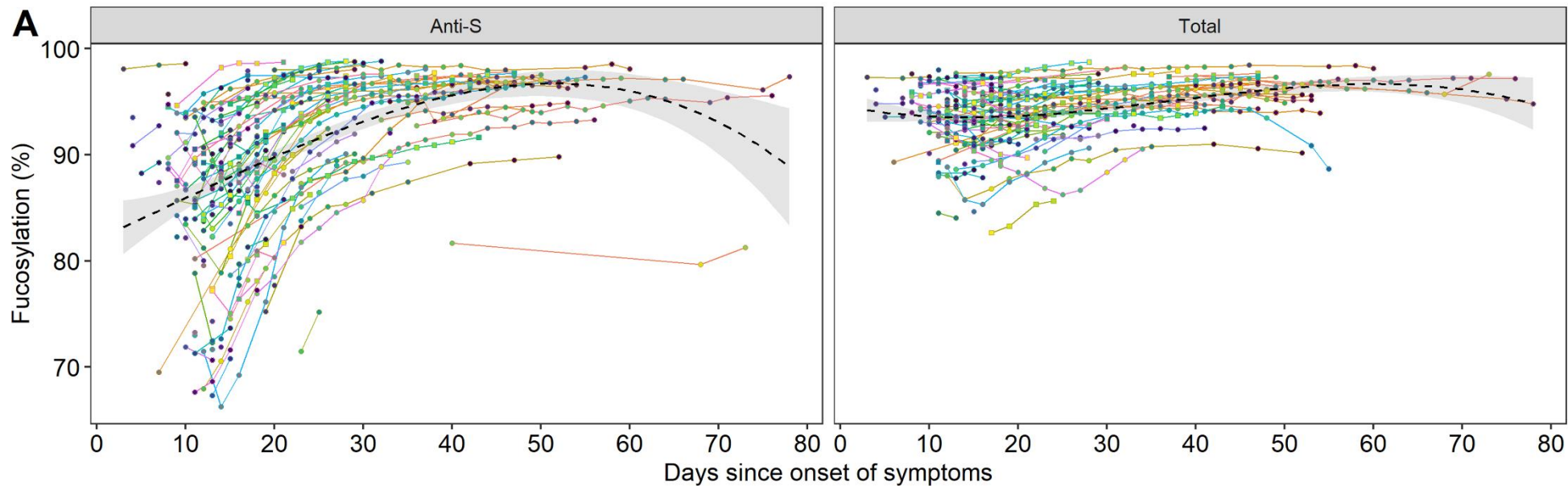
**Supplementary Figure 4.  $\Delta$ IgG1 glycosylation dynamics during the entire hospitalization period.** The time-course of  $\Delta$ glycosylation derived traits (**A**) fucosylation, (**B**) galactosylation, (**C**) bisection and (**D**) sialylation, as shown during hospitalization (n=111). Line colours correspond to a single COVID-19 patient, whilst the colour gradient in the circles/squares indicates the corresponding severity score (grey = NA). The shape displays whether a patient passed away (square) or was discharged alive (circle). The black dashed line with a grey 95% confidence interval band is a cubic polynomial fit over the shown datapoints to illustrate overall dynamics.

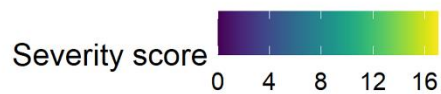
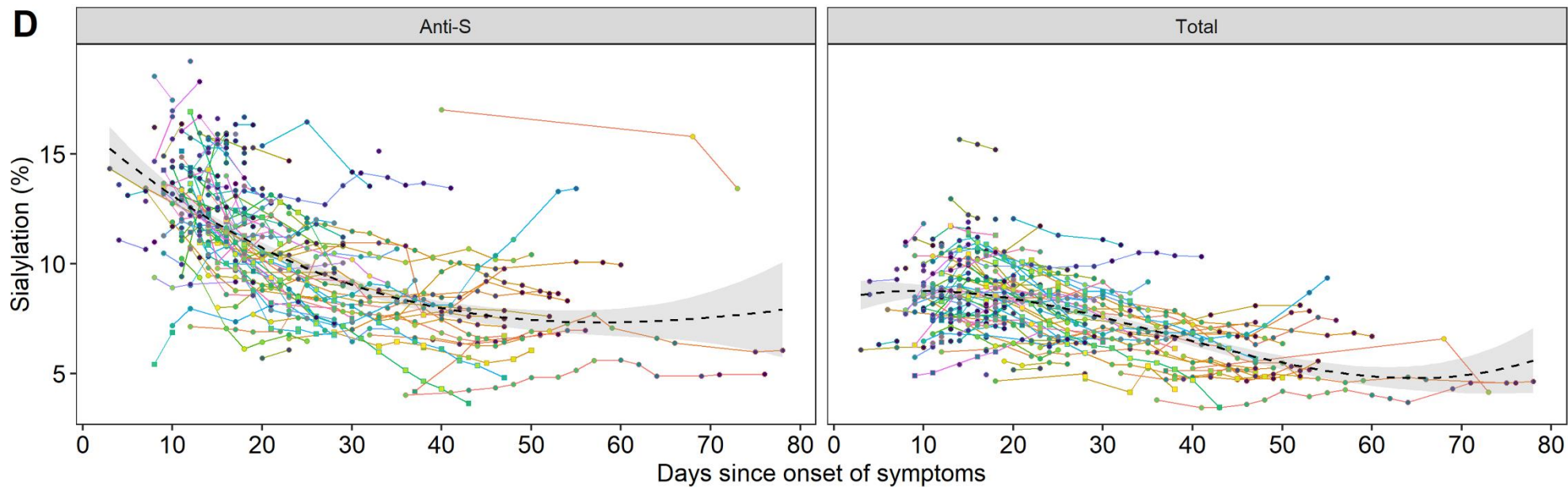
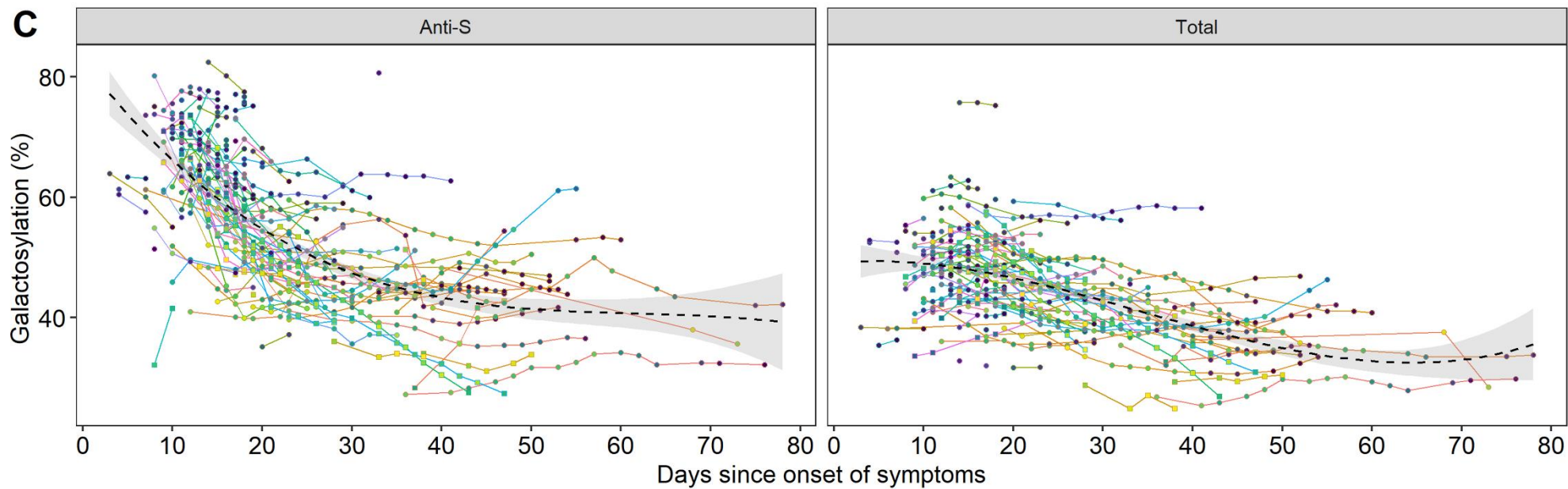




**Supplementary Figure 5.  $\Delta$ IgG1 glycosylation dynamics of the subset of patients with a follow-up sample.**

The time-course of  $\Delta$ glycosylation derived traits (**A**) fucosylation, (**B**) galactosylation, (**C**) bisection and (**D**) sialylation, as shown during the hospitalization period and follow-up (n=19). Line colours correspond to a single COVID-19 patient, whilst the colour gradient in the circles/squares indicates the corresponding severity score (grey = NA). The circle and shape display whether the timepoint corresponds to a follow-up sample (square) or to a sample taken during hospitalization (circle). The black dashed line with a grey 95% confidence interval band is a cubic polynomial fit over the shown datapoints to illustrate overall dynamics.

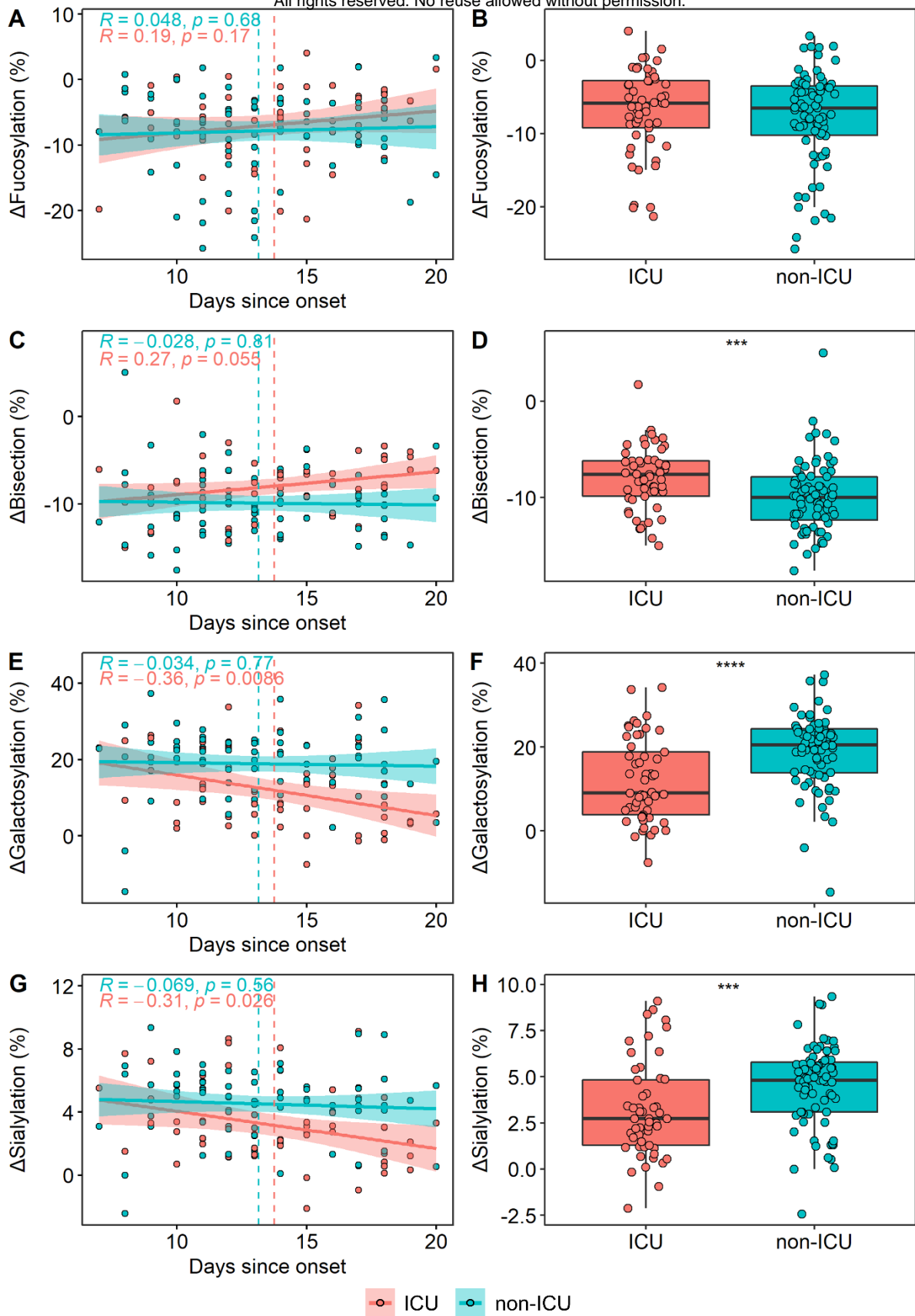




Survival □ Death ○ Discharge

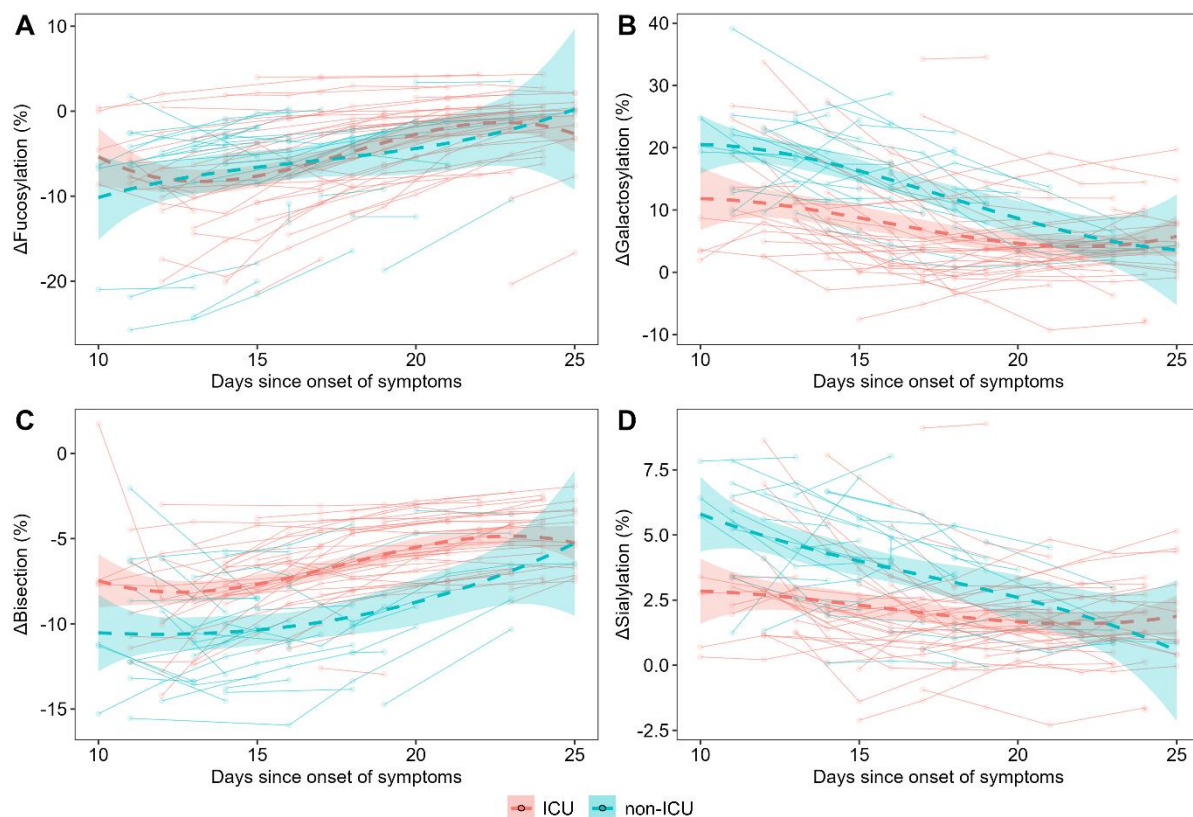
**Supplementary Figure 6. Anti-S and total IgG1 glycosylation dynamics during the entire hospitalization period.** The time-course of glycosylation derived traits **(A)** fucosylation, **(B)** bisection, **(C)** galactosylation and **(D)** sialylation as shown during the hospitalization period (n=111). Anti-S IgG1 dynamics are shown in the left facets, whereas total IgG1 dynamics in the right facets in each panel. Line colors correspond to a single COVID-19 patient, whilst the colour gradient in the circles/squares indicates the corresponding severity score (grey = NA). The circle and shape display whether the patient passed away (square) or was discharged alive (circle) from the hospital. The black dashed line with a grey 95% confidence interval band is a cubic polynomial fit over the shown datapoints to illustrate overall dynamics. Note that the confounding effect of age largely influences the observed bisection **(Figure S2C)**, galactosylation **(Figure S2E)** and **(Figure S2G)** sialylation pattern, thereby has been corrected for age effects **(Figure S2)**.



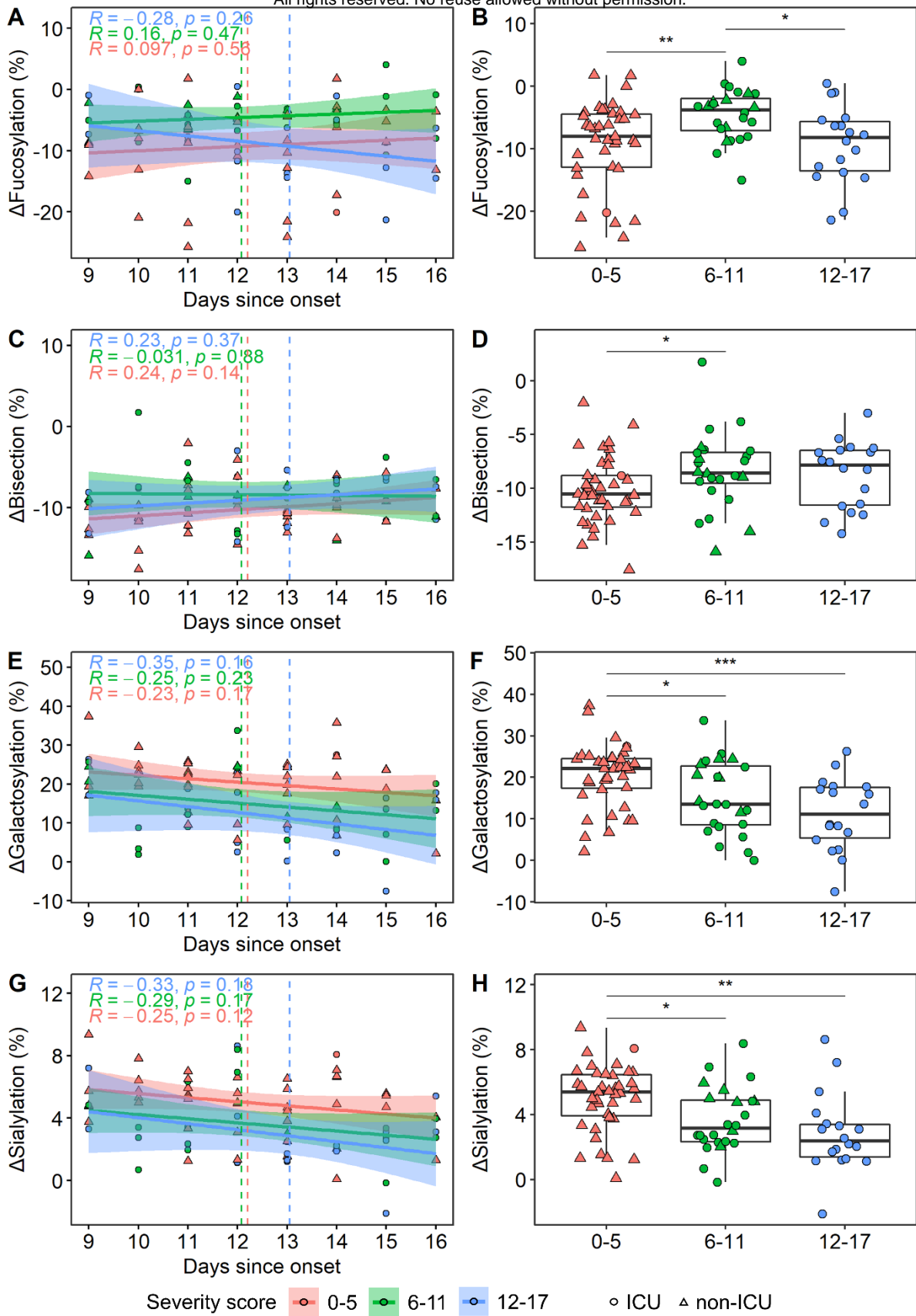


**Supplementary Figure 7. ICU (red) and non-ICU (blue) patients and corresponding  $\Delta$ IgG1 glycosylation derived traits in a “days since onset of symptoms” subset of patients (n=129) to confirm that the observed differences (Figure 3) are not confounded by vast glycosylation dynamics.  $\Delta$ IgG1 (A) fucosylation, (C) bisection, (E) galactosylation and (G) sialylation as a proxy of days since symptom onset. Shown in the inset are**

All rights reserved. No reuse allowed without permission.  
the Spearman correlation coefficients ( $R$ ) and  $p$ -values, respectively. The red (ICU) and blue (non-ICU) lines are linear regression lines and the corresponding band indicates the 95% confidence interval. The dashed vertical lines indicate group means. Comparison of corresponding  $\Delta$ IgG1 (B) fucosylation, (D) bisection, (F) galactosylation and (H) sialylation levels between ICU and non-ICU patients. All datapoints correspond to baseline samples (time of hospitalization).

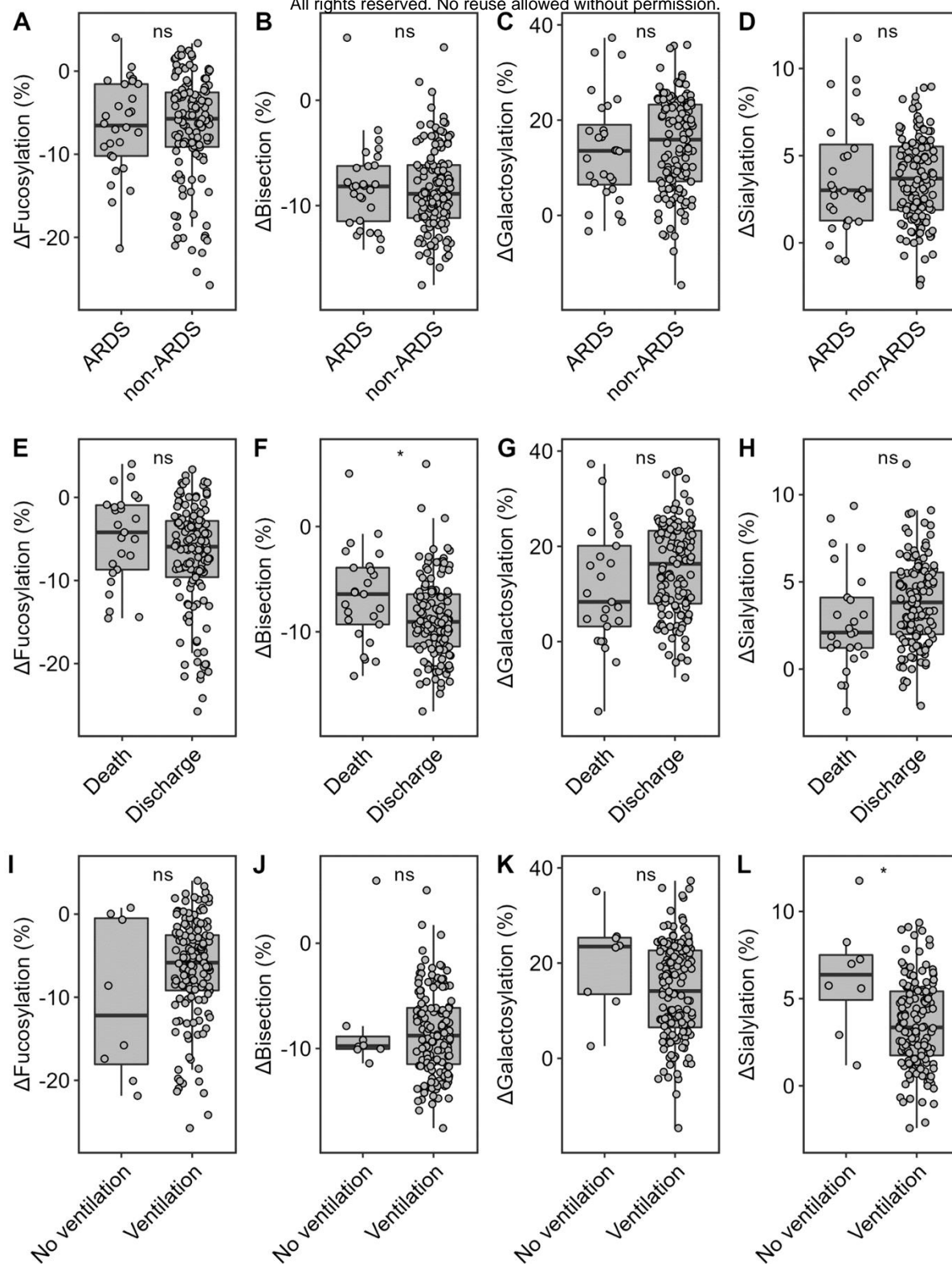


**Supplementary Figure 8.  $\Delta$ IgG1  $\Delta$ glycosylation dynamics of patients admitted to the ICU (n=48; red) and non-ICU (n=34; blue) treatments as shown between days 10 and 25. The time course of  $\Delta$ IgG1 glycosylation traits (A) fucosylation, (B) galactosylation, (C) bisection and (D) sialylation. The dashed lines with 95% confidence interval bands are cubic polynomials fit over the shown datapoints to illustrate overall dynamics.**



All rights reserved. No reuse allowed without permission.

**Supplementary Figure 9. Patients in varying severity score groups 0-5 (red), 6-11 (green) and 12-17 (dark blue) and corresponding  $\Delta$ IgG glycosylation derived traits in a “days since onset of symptoms” subset of patients to confirm that the observed differences (Figure 4) are not confounded by vast glycosylation dynamics.**  $\Delta$ IgG1 (A) fucosylation and (C) bisection, (E) galactosylation and (G) sialylation as a proxy of days since onset of subset of patients. Shown in the inset are the Spearman correlation coefficients (R) and *p*-values, respectively. The red (0-5), green (6-11) and blue (12-17) lines are linear regression lines and the corresponding band indicates the 95% confidence interval. Dashed vertical lines indicate group mean. Comparison of corresponding  $\Delta$ IgG1 (B) fucosylation and (D) bisection, (F) galactosylation and (H) sialylation levels between the three severity score groups. Circle indicates ICU patients, whereas squares indicate non-ICU patients. All datapoints correspond to baseline samples (time of hospitalization).



**Supplementary Figure 10. Comparison of acute respiratory distress syndrome (A-D), survival (E-H) and ventilation (I-L) subgroups of patients for glycosylation traits fucosylation (A, E, I), bisection (B, F, J), galactosylation (C, G, K) and sialylation (D, H, L). Bisection negatively associated with, survival, and sialylation negatively associated with ventilation. No other associations were found.**



medRxiv preprint doi: <https://doi.org/10.1101/2021.11.18.21266442>; this version posted November 20, 2021. The copyright holder for this preprint (which was not certified by peer review) is the author/funder, who has granted medRxiv a license to display the preprint in perpetuity. All rights reserved. No reuse allowed without permission.

### References

1. Gudelj I, Lauc G, Pezer M. Immunoglobulin G glycosylation in aging and diseases. *Cell Immunol* 2018; **333**: 65-79.